



Document Title: **Telescope Structure Finite Element Analysis**

Document Number: **VIS-ANA-VER-01001-0252
(S780-0252)**

Issue: **B**

Date: **28 May 2004**

Document Prepared By:	David W. Adkins, P.E. VertexRSI
Document Interpreted By:	David Finley, P.E. Vertex RSI
Document Approved By:	David Porter Vertex RSI
Document Released By:	David Porter Vertex RSI

The information contained in this document is strictly confidential and is intended for the addressee only. The unauthorised use, disclosure, copying, alteration or distribution of this document is strictly prohibited and may be unlawful.

Change Record

Issue	Date	ECN	Section(s) Affected	Description of Change/Change Request Reference/Remarks
A	19 Aug 03	03-0709	All	Original Release
B	28 May 03	04-0554	All	FDR Update

Table of Contents

1	INTRODUCTION	7
2	ACRONYMS AND ABBREVIATIONS.....	7
3	APPLICABLE AND REFERENCED DOCUMENTS	7
4	ANALYSIS REPORT	8
4.1	SCOPE OF THE ANALYSIS	8
4.2	ASSUMPTIONS	8
4.2.1	<i>Azimuth Bearing Modelling Assumptions</i>	<i>9</i>
4.2.2	<i>Altitude Bearing Interface</i>	<i>11</i>
4.2.3	<i>Altitude Drive Interface</i>	<i>11</i>
4.2.4	<i>M1 Mirror Cell Interface</i>	<i>12</i>
4.3	MODEL	12
4.3.1	<i>Changes to the FEA Model For M2 Analysis</i>	<i>17</i>
4.3.2	<i>Discussion of the Model.....</i>	<i>20</i>
4.4	LOADING CASES	22
4.4.1	<i>General Load Cases Required by Specification</i>	<i>22</i>
4.4.2	<i>Gravity Loads</i>	<i>23</i>
4.4.3	<i>Thermal Loads.....</i>	<i>23</i>
4.4.4	<i>Survival Wind Loads.....</i>	<i>23</i>
4.4.5	<i>Operating Wind Loads</i>	<i>23</i>
4.4.6	<i>Buffer Impact Loads</i>	<i>27</i>
4.4.7	<i>Earthquake Loads</i>	<i>27</i>
4.4.8	<i>M1 Cell Loads.....</i>	<i>31</i>
4.4.9	<i>Component Loads.....</i>	<i>31</i>
4.5	FEA RESULTS	33
4.5.1	<i>FEA Results Summary.....</i>	<i>33</i>
4.5.2	<i>Locked Rotor Frequency.....</i>	<i>34</i>
4.5.3	<i>Mesh Density Error</i>	<i>38</i>
4.5.4	<i>Operating Load Cases, Maximum Stress</i>	<i>39</i>
4.5.5	<i>Survival / Accidental Load Cases, Maximum Stress</i>	<i>45</i>
4.5.6	<i>Platform Motion</i>	<i>52</i>
4.5.7	<i>M1 to M2 Motion from Wind</i>	<i>53</i>
4.6	COMPONENT RESULTS.....	54
4.6.1	<i>Cassegrain Bearing</i>	<i>54</i>
4.6.2	<i>Altitude Bearings.....</i>	<i>55</i>
4.6.3	<i>Foundation Interface.....</i>	<i>56</i>
4.6.4	<i>Azimuth Bearing</i>	<i>56</i>
4.6.5	<i>Component Interfaces.....</i>	<i>56</i>
5	APPENDIX.....	57

TABLE OF FIGURES

FIGURE 1 - FINITE ELEMENT MODEL OF VISTAMOUNT	9
FIGURE 2 - CROSS SECTION VIEW OF AZIMUTH BEARING IN MOUNT MODEL.....	10
FIGURE 3 - FEA MODEL OF OSS SYSTEM	12
FIGURE 4 - FEA MODEL OF M2 SUPPORT STRUCTURE	13
FIGURE 6 - FEA MODEL OF ALTITUDE RING	14
FIGURE 7 - FEA MODEL OF M1 ASSEMBLY	15
FIGURE 8 - FEA MODEL OF YOKE	15
FIGURE 9 - FEA MODEL OF ALTITUDE BEARING HOUSINGS	16
FIGURE 10 - FEA MODEL OF AZIMUTH BEARING	16
FIGURE 11 - FEA MODEL OF PEDESTAL ASSEMBLY	17
FIGURE 12 - M2 ASSEMBLY WITH XY VANE CONFIGURATION	18
FIGURE 13 - M2 CONFIGURATION WITH TANGENTIAL VANE CONFIGURATION	18
FIGURE 14 - M2 ASSEMBLY WITH 5 VANE CONFIGURATION	19
FIGURE 15 - ALTITUDE LOCKED ROTOR RESONANCE	24
FIGURE 16 - ALTITUDE LOCKED ROTOR RESONANCE	35
FIGURE 17 - AZIMUTH LOCKED ROTOR RESONANCE.....	36
FIGURE 18 - M2 LOCKED ROTOR RESONANCE	37
FIGURE 19 - MESH DENSITY ERROR FOR MOUNT FEA MODEL	38
FIGURE 20 - STRESS PLOT FOR LOAD COMBINATION A	40
FIGURE 21 - STRESS PLOT FOR LOAD COMBINATION B	41
FIGURE 22 - STRESS PLOT FOR LOAD COMBINATION C	42
FIGURE 23 - STRESS PLOT FOR LOAD COMBINATION D	43
FIGURE 24 - STRESS PLOT FOR LOAD COMBINATION E.....	44
FIGURE 25 - STRESS PLOT FOR LOAD COMBINATION 1 - 1.....	46
FIGURE 26 - STRESS PLOT FOR LOAD COMBINATION 1 - 2.....	47

Doc Number:	VIS-ANA-VER-01001-0252 (S780-0252)
Date:	28 May 2004
Issue:	B
Page:	5 of 79
Author:	D. Adkins

FIGURE 27 - STRESS PLOT FOR LOAD COMBINATION 1 - 3.....	48
FIGURE 28 - STRESS PLOT FOR LOAD COMBINATION 2 - 1.....	49
FIGURE 30 - STRESS PLOT FOR LOAD COMBINATION 2 – 3	51
FIGURE 31 – PLATFORM LOCATION.....	52

TABLE OF TABLES

TABLE 1 - LOAD COMBINATIONS FOR MOUNT ANALYSIS	22
TABLE 2 – EFFECTIVE MASSES FOR PSD ANALYSIS	27
TABLE 3 – OBE 1% ACCELERATION RESPONSE SPECTRUM	28
TABLE 4 – MLE 1% ACCELERATION RESPONSE SPECTRUM.....	28
TABLE 5 – EFFECTIVE MASSES FOR RESPONSE ANALYSIS	29
TABLE 6 – LOCATION OF ACCELERATION NODES	29
TABLE 7 –MLE ACCELERATION RESULTS	30
TABLE 8 –MLE ACCELERATION INPUTS TO FEA	31
TABLE 9 –MLE ACCELERATION INPUTS FOR M1 CELL.....	31
TABLE 10 –MLE ACCELERATION INPUTS FOR M2.....	32
TABLE 11 –MLE ACCELERATION INPUTS FOR CASSEGRAIN	32
TABLE 12 –MLE ACCELERATION INPUTS FOR ALTITUDE BEARINGS	32
TABLE 13 - SUMMARY OF RESULTS.....	33
TABLE 14 - FIRST NATURAL FREQUENCIES OF MOUNT	34
TABLE 15 - RESULTS FOR OPERATING LOAD CASES	39
TABLE 16 - RESULTS FOR SHORT TERM ACCIDENTAL LOAD CASES	45
TABLE 17 - RESULTS PLATFORM MOTION	52
TABLE 18 - M1 – M2 MAXIMUM DISPLACEMENTS	53
TABLE 19 - M1 – M2 CORRELATED DISPLACEMENTS	53
TABLE 20 – CASSEGRAIN ACCELERATIONS.....	54
TABLE 21 – CASSEGRAIN BEARING RESULTS	54
TABLE 22 – ALTITUDE BEARING INPUT LOADS	55
TABLE 23 – ALTITUDE BEARING RESULTS	55
TABLE 24 – FOUNDATIO N RESULTS.....	56

1 Introduction

This analysis presents the results of the finite element analysis of the Vista mount. This document shows the telescope mount meets the performance requirements in the specification.

2 Acronyms and Abbreviations

ADXX	Applicable Document XX
FE	Finite Element
FEA	Finite Element Analysis
IR	Infrared
MLE	Maximum Likely Earthquake
OBE	Operating Basis Earthquake
OSS	Optical Support Structure
PSD	Power Spectral Density
VER	VertexRSI
VIS	VISTA
TRE	Technical Report

3 Applicable and Referenced Documents

Number	Title	Number & Issue
AD01	Statement of Work for the VISTA Telescope Work Package	VIS-SOW-ATC-01000-0005 Issue 2.0, 21 Feb. 2003
AD02	Technical Specification for the Telescope Structure Work Package	VIS-SPE-ATC-01000-0006 Issue 3.0, 21 Feb. 2003
AD03	Statement of Work for the Structural Analysis of the VISTA Telescope Mount	S780-0810, Rev. A 05 May 2003
AD04	VLT Environmental Specification	VLT/SPE/ESO/10000/0004 Issue 6, 12 Nov. 1997
AD05	Telescope Mount Design Report-Structures	VIS-TRE-VER-01001-0707 S780-0707 Rev A
AD06	Finite Element Model of Vista Mount	S780-0251-A
AD07	M1 Mirror Cell Analysis Report	VIS-ANA-VER-03001-0260 S780-0260-C
AD08	Earthquake Analysis Report	VIS-TRE-VER-01001-0700-E (S780-0700)
AD09	Not used	
AD10	Drive Analyses	VIS-ANA-VER-01001-0254-C (S780-0254-D)

AD11	M1 Cell FEA	S780-260-C
AD12	Weight and Centre of Gravity Analysis	VIS-ANA-VER-01001-0250 (S780-0250-E)
AD13	Pointing and Tracking Analysis	VIS-TRE-01001-9001 Issue 2.0
AD14	Halbeck Analysis on Azimuth Gearbox Stiffness	S780-7495-B
AD15	Euro code 8: Design Provisions for Earthquake Resistance of Structures	DD ENV 1998 – 1:1996

4 Analysis Report

4.1 Scope of the Analysis

The purpose of this analysis is to demonstrate by analysis the Vista mount meets the specification requirements, AD02. It does not include the static deflections of the OSS, which is in report AD07.

4.2 Assumptions

The Vista FEA model is shown in Figure 1. Several assumptions were made during the development of the FEA model for the Vista analysis. These were made primarily due to the nature of the design process. The following discusses the assumptions that were made.

The M1 mirror cell model was combined with the mount FEA for seismic, resonance, and deflection analysis. The M2 mirror was modelled as a concentrated mass, which included both the mass and inertia of the mirror. This concentrated mass is located at the centre of gravity of the mirror. The IR camera was modelled as a concentrated mass, which included inertia. The foundation and properties of the soil were included for seismic analysis as well. For resonance analysis purposes, the mount was supported at the base, which assumes a rigid foundation as directed by AD02.

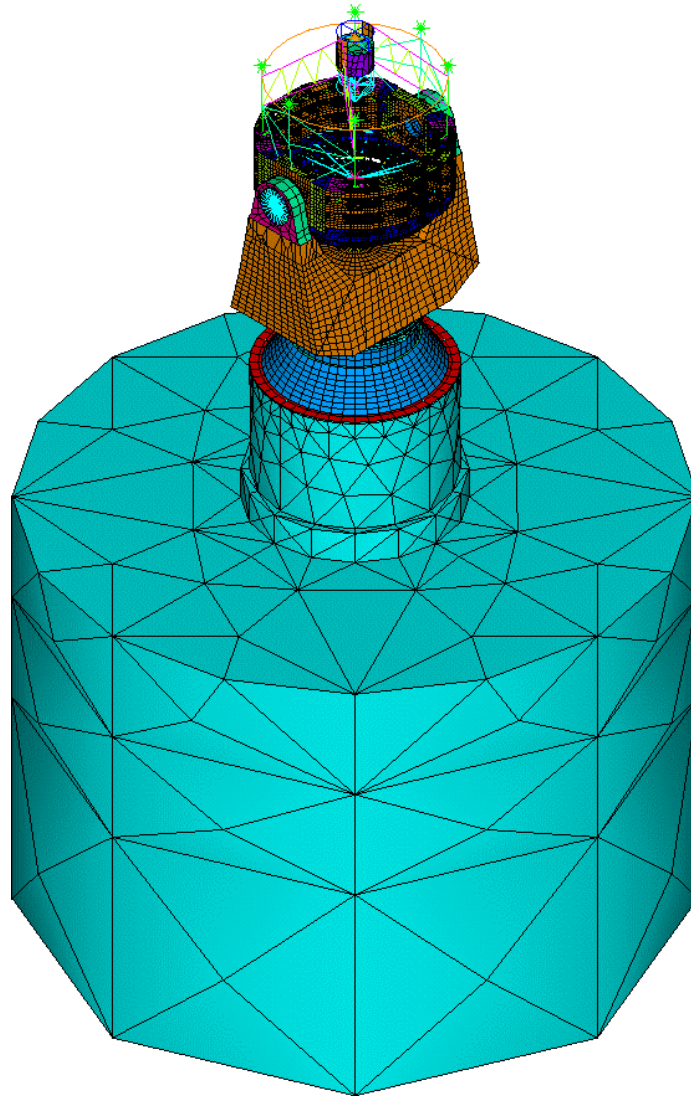


Figure 1 - Finite Element Model of Vista Mount

4.2.1 Azimuth Bearing Modelling Assumptions

The cross section of the azimuth bearing is shown in Figure 2. The azimuth bearing has two sets of rolling elements. The first set, the larger of the two, is designed to carry thrust load and provide the overturning and thrust stiffness of the bearing. The second set of rolling elements is smaller and provides the radial stiffness of the bearing. The cross section is designed to assure the radial elements do not carry thrust load and the thrust elements do not carry radial load.

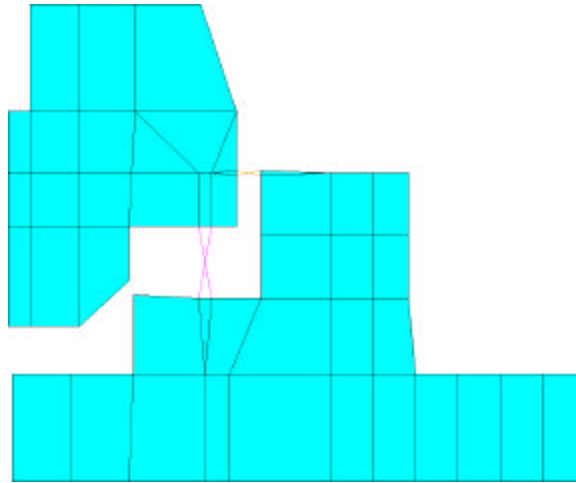


Figure 2 - Cross Section View of Azimuth Bearing in Mount Model

The azimuth bearing raceways are modelled using solid elements, as are the interface plates between the bearing and the rest of the structure. The rest of the structure is modelled using shell elements. The solid elements support 3 degrees of freedom per node, while the shells support 6. The interface between the two is accomplished by using a layer of thin shell elements that covers the face of the solid elements where they meet the shells. These elements assure moment transfer between the shell and solid elements. The translational loads are carried directly between the solid and shell elements.

The rolling elements of the azimuth bearing are modelled using truss elements. The truss elements and the solid elements do not support rotation at their nodes, thereby allowing bearing rotation. The spring stiffness representing the azimuth drives restrains bearing rotation.

The bearing vendor supplied the stiffnesses of the rolling elements. The stiffnesses are nonlinear with respect to the load, as it is a function of the contact surface between the rolling element and the raceway. The vendor determined the stiffnesses using industry standard software, based on overall bearing loads supplied by VRSI.

It was necessary to convert from the overall stiffness of the bearing (as supplied by the vendor) into individual element stiffness that would collectively match the overall number. As a check on that calculation, the element stiffnesses were applied to a copy of the FEA model. Everything in the model other than the azimuth bearing elements had its Young's modulus increased by a factor of 10^6 . Simple loads were applied to this test model and the deflections were measured and compared to hand calculations. The stiffness of the spring elements was adjusted to make the actual deflections match hand calculations.

Doc Number:	VIS-ANA-VER-01001-0252 (S780-0252)
Date:	28 May 2004
Issue:	B
Page:	11 of 79
Author:	D. Adkins

The azimuth drive stiffness is modelled using spring elements. The gearbox vendor, based on his system analysis, supplied the stiffnesses. The spring stiffness was based on the stiffness of the gear mesh and the output pinion shaft and bearings. The calculations for the azimuth drive stiffnesses were done in AD14.

4.2.2 Altitude Bearing Interface

The bearing vendor determined the stiffness of the altitude bearings. The stiffness to load relationship is nonlinear, being a function of the contact area between the rolling element and the raceway. The bearing vendor determines the stiffness based on loads supplied by VRSI.

The bearings are modelled as spring elements that match the stiffness supplied by the vendor. Each altitude bearing was actually 24 spring elements arranged in a radial pattern between the altitude axle and the altitude bearing housing on the yoke. It was necessary to convert from the overall stiffness of the bearing (as supplied by the vendor) into individual element stiffnesses that would collectively match the overall number. As a check on that calculation, the element stiffnesses were applied to a copy of the FEA model. Everything in the model other than the altitude bearing elements had their Young's modulus increased by a factor of 10^6 . Simple loads were applied to this test model and the deflections were measured and compared to hand calculations. The stiffness of the spring elements was adjusted to make the actual deflections match hand calculations.

4.2.3 Altitude Drive Interface

The altitude drive motors are direct drive motors, with no gear mesh providing drive stiffness. The action of the motor provides a type of stiffness for the system, but not a mechanical stiffness. The motor stiffness was treated differently depending on the type of analysis.

For locked rotor resonance (LRR) analysis, there was no stiffness between the stator and rotor. This decouples the rotating inertia between the OSS and the yoke. Putting a zero value stiffness between two parts of the FEA model creates a singularity, which will abort the solution. The model has a very low stiffness rotational spring between the OSS and the yoke. The first mode from this analysis is a rotation of the OSS about the altitude axis, involving the inertia of the OSS and the stiffness of the rotational spring. This is an artificial mode and is discarded, an artefact of the FEA.

The first mode with physical significance is the second mode, which is a nodding mode. The yoke arms oscillate perpendicular to the altitude axis, while the OSS stays level and travels with the top of the yoke arms. This motion is consistent with a mode where the motor has been decoupled from the inertia it is driving, consistent with a locked rotor resonance.

For a seismic and wind analysis, the OSS and the yoke are coupled through the drive because it is under active servo control. This could be either through the brake or the action of the motor torque itself. This torsional moment of inertia of drive motor is $I_{xx} = 270 \times 10^{-6} \text{ m}^4$.

4.2.4 M1 Mirror Cell Interface

The M1 cell model was combined with the mount model for this analysis. The assumptions used in deriving that model are described in AD07.

Using the M1 cell model in the overall FEA means model provides a better representation of the stiffness between the M1 cell and the altitude ring.

4.3 Model

The mount was modelled using Ansys, a general purpose finite element program. Ansys was used to perform a linear static analysis for displacements, a modal analysis for finding natural frequencies, a response spectral for earthquakes, and a PSD for wind. Models of the components are shown in Figures 3 through 11.

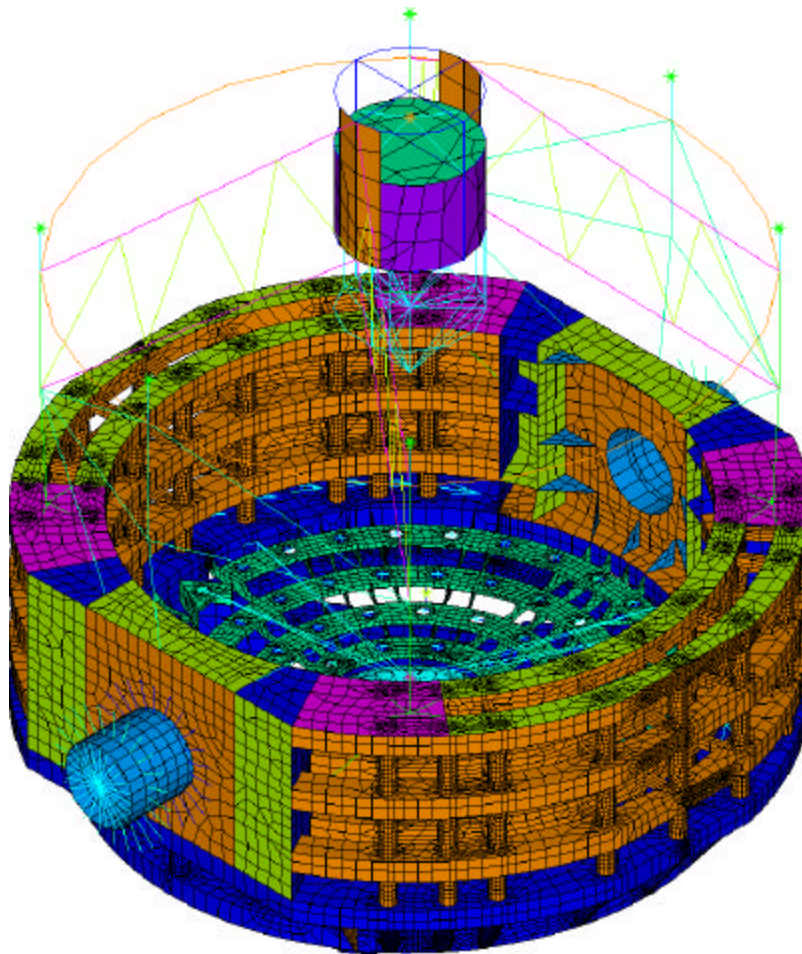


Figure 3 - FEA Model of OSS System

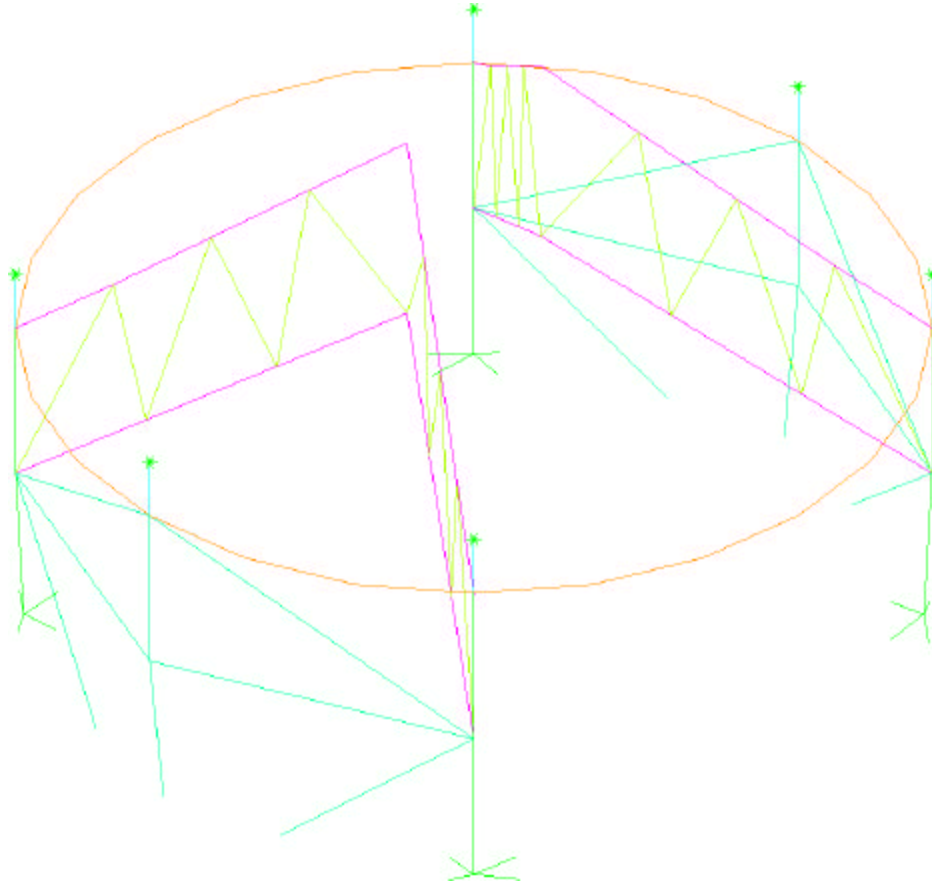


Figure 4 - FEA Model of M2 Support Structure

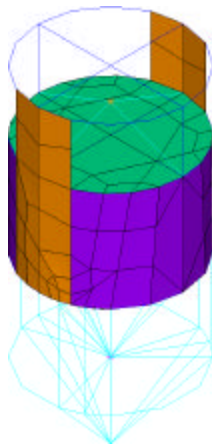


Figure 5 - FEA Model of M2 Assembly

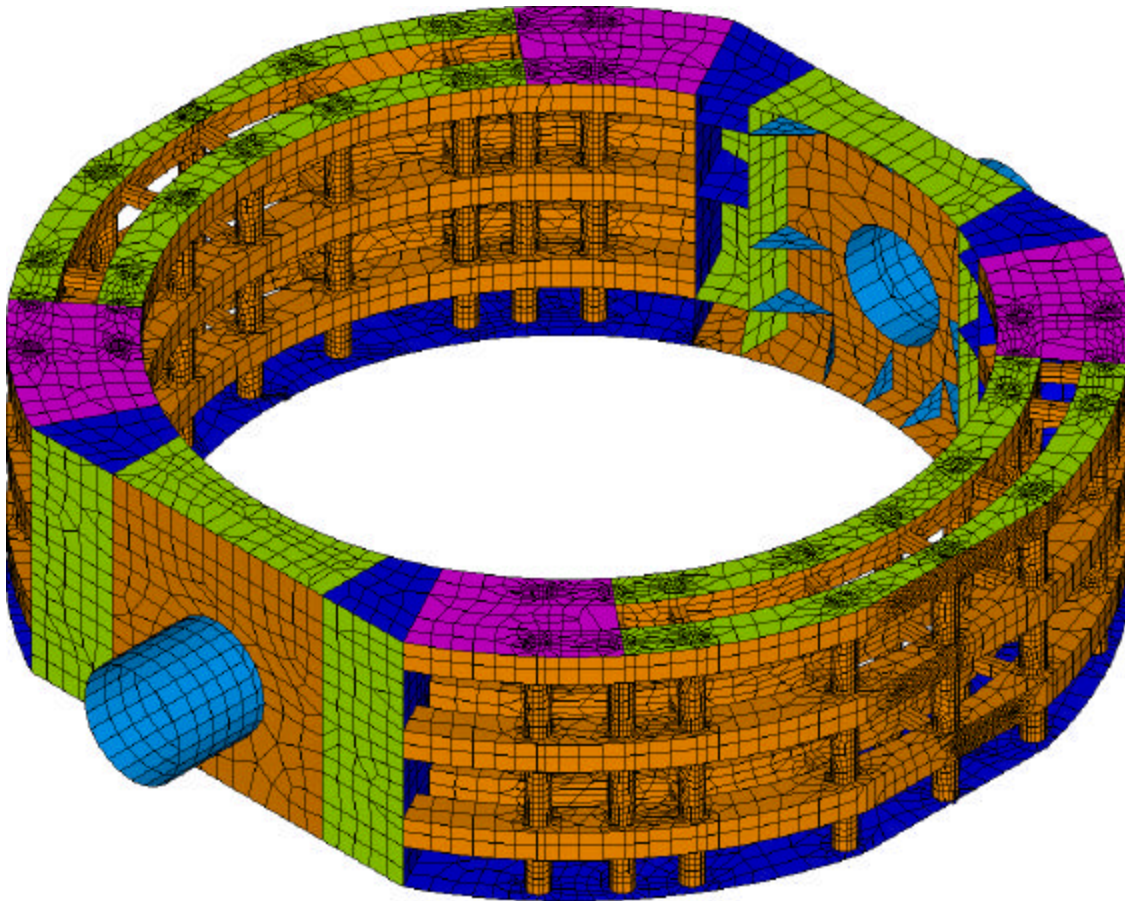


Figure 6 - FEA Model of Altitude Ring

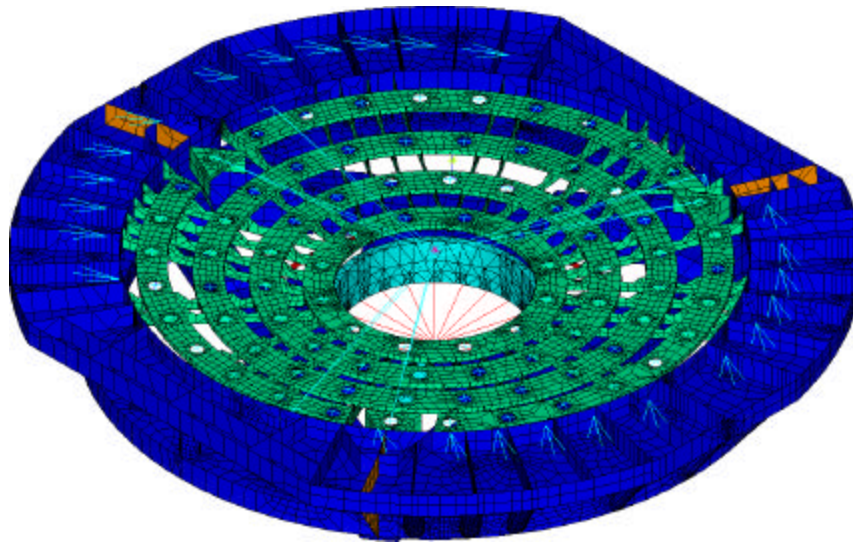


Figure 7 - FEA Model of M1 Assembly

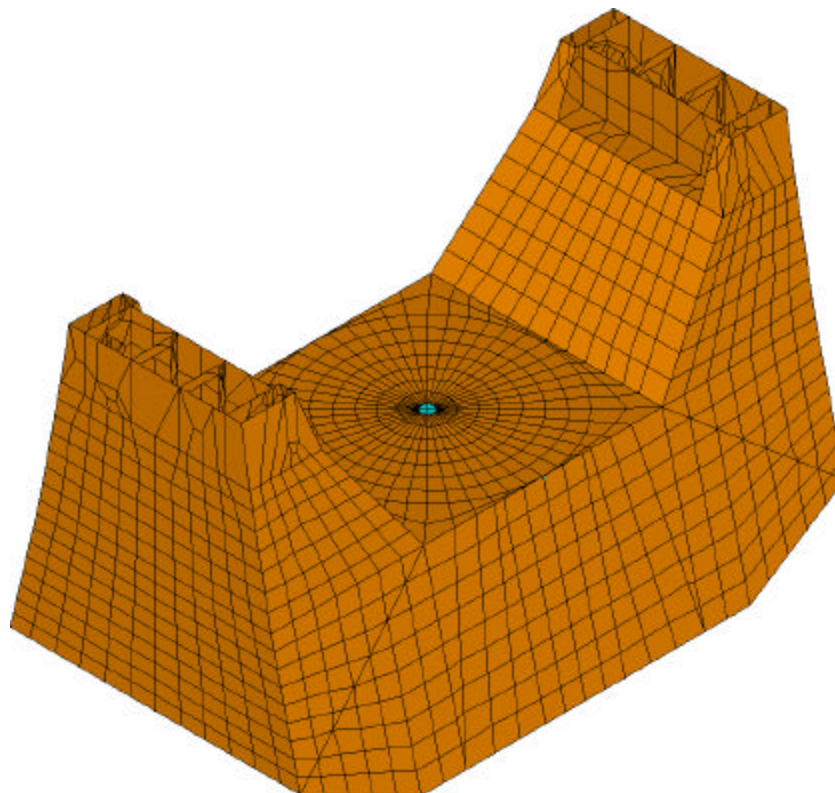


Figure 8 - FEA Model of Yoke

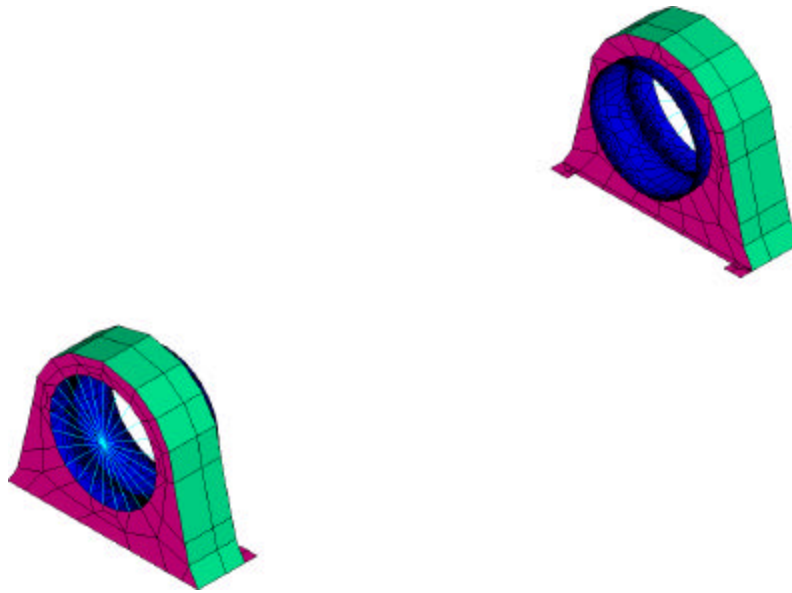


Figure 9 - FEA Model of Altitude Bearing Housings

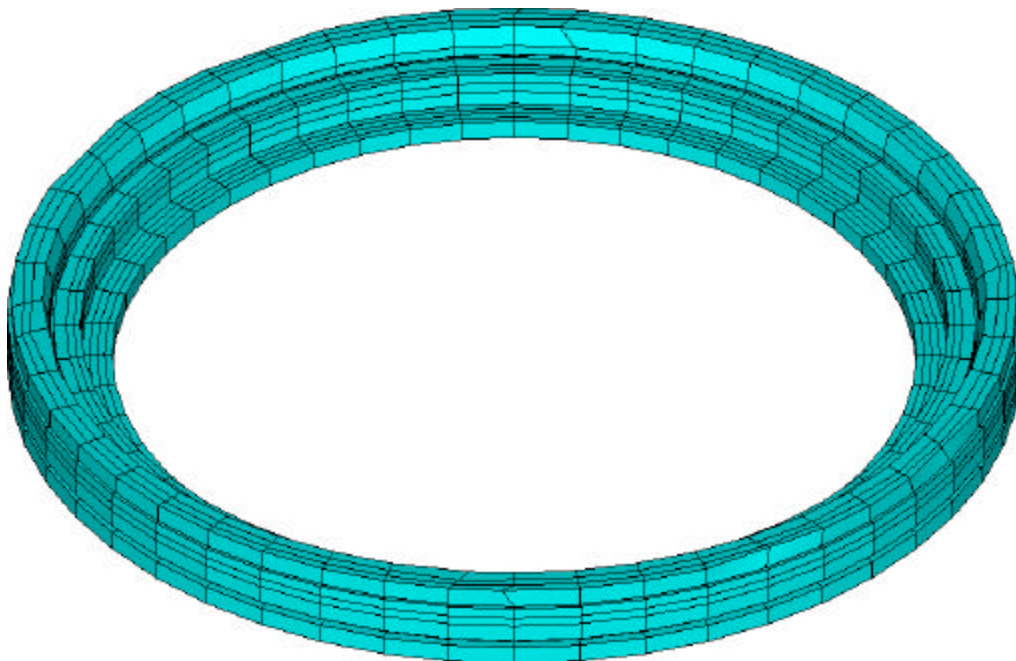


Figure 10 - FEA Model of Azimuth Bearing

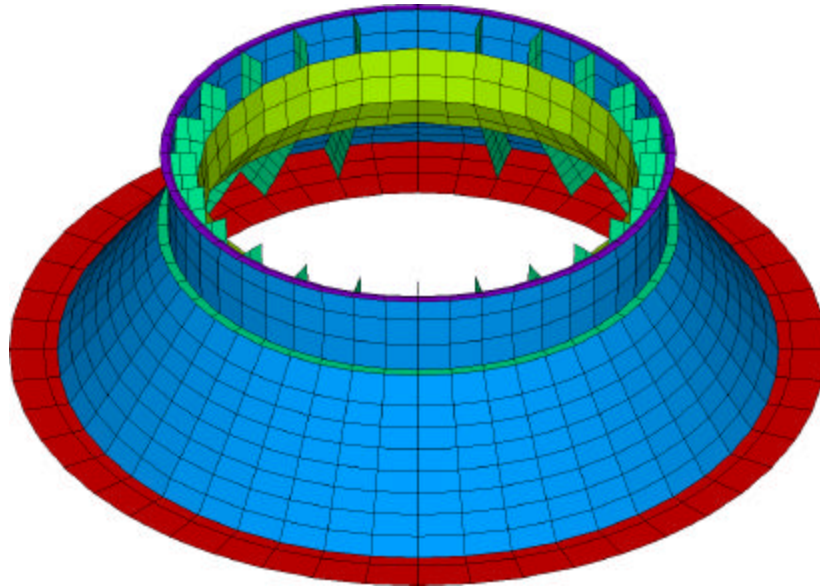


Figure 11 - FEA Model of Pedestal Assembly

4.3.1 Changes to the FEA Model For M2 Analysis

This section outlines the changes to the model in order to support the requirements for the design of M2. The design of M2 was controlled by the following requirements:

1. The vertical stiffness of the M2 assembly must be $\geq 1.3 \times 10^8$ N/m.
2. The repeatable deflections between M1 and M2 should be less than the values given in Table 7 in the specification, AD02.
3. When loaded with the PSD representing the wind loading, the structure deflections support the overall pointing and tracking accuracy requirements.

The original M2 support structure had vanes laid out in a 0° and 90° pattern, with the vanes perpendicular to each other, as shown in Figure 12.

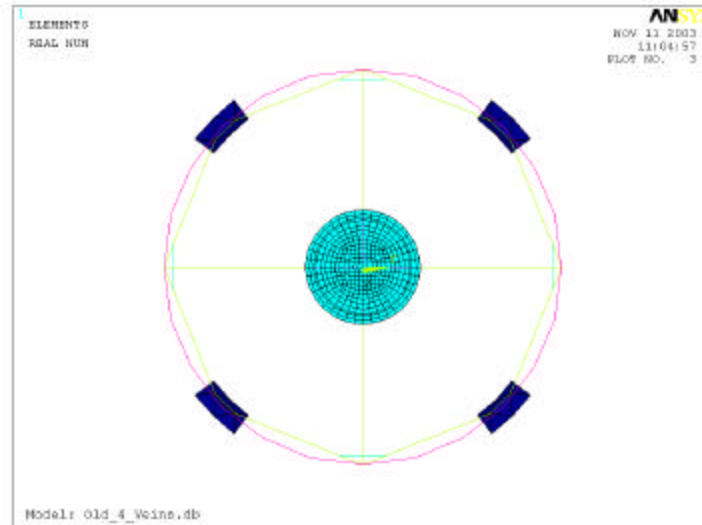


Figure 12 - M2 Assembly with XY Vane Configuration

This truss was deepened to deal with the low natural frequencies caused by the mass of M2. When first loaded with the VISTA M2 instrument, the original configuration had a low torsional frequency, where M2 was twisting about the optical axis. The second approach was a tangential vane approach, where the vanes intersected the M2 support tangentially to its surface, as shown in Figure 13. This approach solved the torsional mode problem, but did little to keep the overturning modes under control.

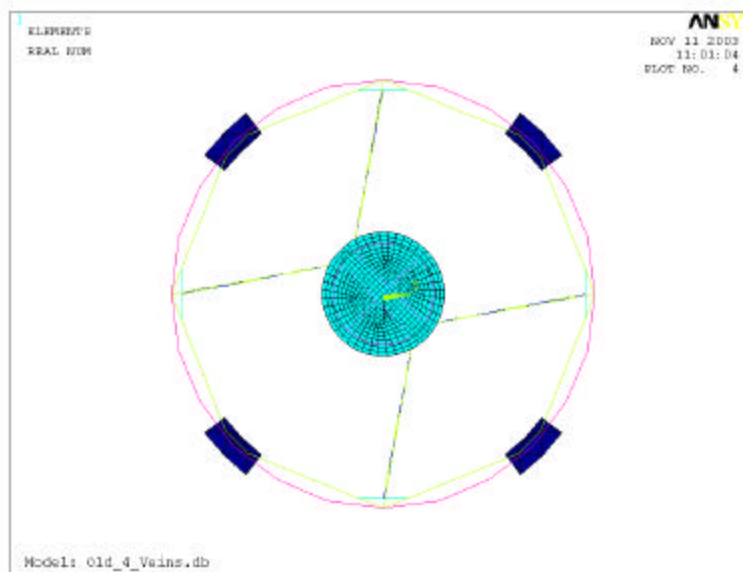


Figure 13 - M2 Configuration with Tangential Vane Configuration

A five vane configuration solved both problems. With this approach, the 0° and 90° vanes were restored, but one was split in half, as shown in Figure 14. This split vane was placed tangential to the surface of the M2 instrument support. The split vane provided torsional resistance, but was still perpendicular to the other vanes, and therefore could handle the overturning oscillation about the altitude axis.

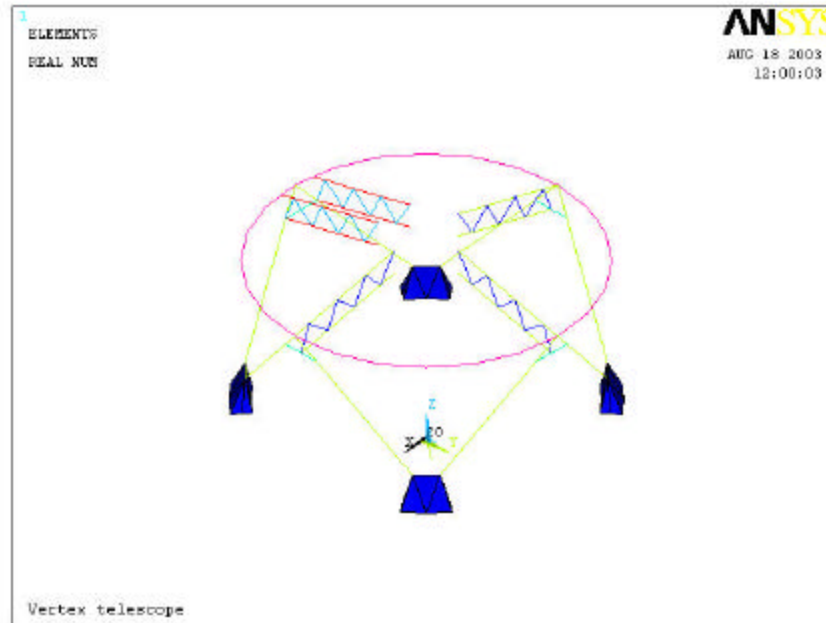


Figure 14 - M2 Assembly with 5 Vane Configuration

Unfortunately, the five vane configuration did not work from an optical standpoint. It is necessary to keep the number of vanes to a minimum and four vanes appear to be the limit the optical performance can tolerate. The XY vane configuration appeared to be the best option.

As the design progressed, additional requirements forced a change in approach. The requirements for stiffness along the optical axis and the wind loading PSD began to point to the tangential vane option as the best option, especially with deeper vanes. The tangential vane option alone increased the torsional stiffness of the M2 Assembly. Increasing the depth of the trusses stiffened them for axial stiffness and for the alt LRR. In addition, sloping the trusses, achieved by moving the M2 ring closer to the altitude ring, increased the axial stiffness. Increasing the stiffness about these two axes also decreased the PSD response of the M2 mirror, resulting in lower values to compare to the pointing error budget. The Results Section gives the final design values achieved by these changes.

4.3.2 Discussion of the Model

The element types used in the analysis are briefly discussed below:

- SHELL63 A three-dimensional general purpose shell element with three or four nodes each having six structural degrees of freedom. Input properties include thicknesses at each node.
- BEAM4 A two-noded three-dimensional general purpose beam element having six structural degrees of freedom. Input properties include cross-sectional area, torsional constant, and moments of inertia about two perpendicular axes.
- MASS21 A concentrated three-dimensional concentrated mass element with six structural degrees of freedom. Input properties include the mass concentrated at the element, and mass moments of inertia about each of the coordinate axes.
- COMBINE14 A spring-damper element having longitudinal or torsional properties in one, two, or three dimensions.
- SOLID45 A three-dimensional general-purpose solid element with four, six or eight nodes each having three structural degrees of freedom. No input properties are required for this element.
- LINK8 A three-dimensional uniaxial tension-compression element with three degrees of freedom. Input properties required are the area.

The following material properties were used for the analysis:

Steel:

Young's Modulus	$E = 200 \text{ GPa}$
Poisson's Ratio	$\nu = 0.3$
Density	$\rho = 8,330 \text{ kg/m}^3$ (Includes welds & additional distributed mass)

M1 Mirror:

As given in AD07	5520 kg
Centre of Gravity	-0.63382 m below the Altitude Axis

M2 Unit w/ Mirror:

Mass:	1000 kg
Centre of Gravity	2.03544 m above the Altitude Axis

Doc Number:	VIS-ANA-VER-01001-0252 (S780-0252)
Date:	28 May 2004
Issue:	B
Page:	21 of 79
Author:	D. Adkins

IR Instrument:

Mass: 2900 kg
Centre of Gravity -1.41442 m below the Altitude Axis

The load cases used for the analysis require the OSS to be oriented at different altitude angles. In order to achieve this, it was necessary to hold the OSS still in the global coordinate system and move the mount and foundation. This was necessary because of the loads in the M1 cell that were used to represent the pneumatic actuators. It is less likely to create an error by moving just one load, such as the acceleration due to gravity, than all the loads in the M1 cell.

4.4 Loading Cases

4.4.1 General Load Cases Required by Specification

The load cases given in the specification are outlined in Table 1. An explanation of the derivation of loads for each load cases is given in the following sections. Load Cases A through E are directly from Section 14.1.3 of AD02. However, Load Case 1 and 2 are combinations of Load Cases F through M in the same section.

Table 1 - Load Combinations for Mount Analysis

Category	Operating: Optical Performance			Operating: Stress		Survival / Accidental			
	A	B	C	D	E		1	2	
Alt = 94							X		
Alt = 92					X				
Alt = 88	X								
Alt = 20		X							
Alt = 50			X						
Alt = -2				X					
Alt = -4								X	
Operating Thermal	X	X	X						
Functional Thermal				X	X		X	X	
Operating and Dynamic Wind	X	X	X	X	X				
Survival Wind							X	X	
Buffer							X	X	
OBE									
MLE M1 Cell	X	X	X	X	X		X	X	

The stress results from the MLE meet the requirements of the OBE loads; therefore, the OBE loads were not used in the overall mount stress work. The OBE loads were used in the Azimuth Bearing and Foundation Interface analyses.

4.4.2 Gravity Loads

In order to determine the dead weight behaviour of the mount at various OSS angles, it was necessary to rotate the model of the OSS with respect to the mount. For this analysis, we kept the OSS constant with respect to the global coordinate system and the mount and foundation were moved. This allowed analysis of the OSS at different altitude angles without major changes in the M1 cell load input.

The Operating Load cases, both the Optical Performance and the Stress, used forces to represent the mirror. As explained previously, these forces are from the actuators reacting on the M1 Cell. The mass moment of inertia of the mirror is not in the system. However, for the Short Term Accidental and the Survival, the mirror was represented by a concentrated mass, which included the complete mass properties of the mirror.

4.4.3 Thermal Loads

The thermal loads represent the temperature change over a viewing night. A uniform temperature increase of 15° C was used for the Optical Performance load cases and a uniform increase of 30° C was used for all the other load cases.

4.4.4 Survival Wind Loads

The survival wind loads are based on a wind speed of 36 m/s from Section 6.3.2.3 of AD02. The individual wind forces are based on the size and shape of the component exposed to the wind and placed in the model as concentrated loads.

4.4.5 Operating Wind Loads

The operating wind loads are based on Section 6.3.2.3 and Section 14.1.1.2 of AD02. The operating wind speed of 9 m/s and a 2 m/s rms wind speed. The following paragraphs describe the method used to determine the relative motion of the M1 to the M2 using the PSD method.

The wind velocity is of the form

$$V = \bar{V} + v$$

$$\bar{V} = \text{Mean wind velocity}$$

$$v = \text{Random velocity component representing the wind fluctuation about } \bar{V}.$$

The random velocity component, v , is represented by the von Karman velocity Power Spectral Density (PSD) by the following equation and Figure 15 shows the resulted graph.

$$S(f) = \frac{4 \times \bar{s}^2 \times \left(\frac{L}{\bar{V}}\right)}{\left[1 + 70.8 \times \left(\frac{fL}{\bar{V}}\right)^2\right]^{\frac{5}{6}}}$$

$S(f)$ = Wind velocity spectral density $\frac{(m/s)^2}{Hz}$

\bar{V} = 9 m/s

\bar{s} = RMS wind velocity = 2.0 m/s

L = Scale of Turbulence = 0.6 m

f = Frequency in Hz

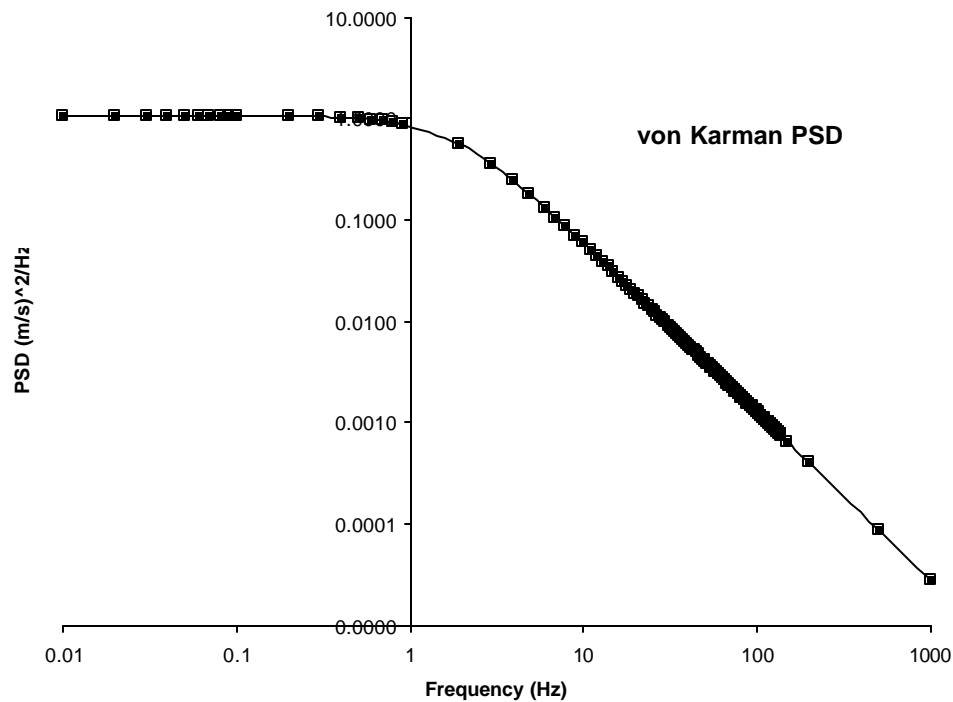


Figure 15 - Altitude Locked Rotor Resonance

The drag force induced by the wind (per unit area) can be expressed by

$$F = C_D \left(\frac{1}{2} \rho V^2 \right)$$

C_D = Drag Coefficient

ρ = Air Density, 1.225 kg/m³.

Using the above formula, the drag force becomes

$$\begin{aligned}
 F &= C_D \frac{1}{2} \rho (\bar{V} + v)^2 \\
 &= C_D \frac{1}{2} \rho (\bar{V}^2 + 2\bar{V}v + v^2) \\
 &= C_D \frac{1}{2} \rho \bar{V}^2 + C_D \rho \bar{V}v + C_D \frac{1}{2} \rho v^2 \\
 &\approx C_D \frac{1}{2} \rho \bar{V}^2 + C_D \rho \bar{V}v \quad (\text{Dropping the last insignificant term})
 \end{aligned}$$

Here, the first term is a constant but the second term represents the random forces from the wind: $C_D (11.025v)$.

In order to estimate the drag coefficients C_D , calculate the Reynolds Number,

$$\begin{aligned}
 R_e &= \frac{\rho V L}{\mu} \\
 &= \frac{1.225 \times 9 \times 5}{1.8 \times 10^{-5}} \quad (L = 5 \text{ m, Diameter of the structure}) \\
 &= 3.0625 \times 10^6
 \end{aligned}$$

Based on this value of R_e , indicating turbulent flow, the C_D values can be obtained from a fluid mechanics table.

Combining with the von Karman PSD, the random force PSD is now obtained. The force PSD is applied to the structure on the areas facing the wind. The spectrum analysis generates the standard deviations (1 σ displacements or RMS) of all nodes in the model along with the covariance for any two nodes.

The distance between the M1 vertex and the M2 vertex is 2.72486 m. Any deviation of M2 relative to M1 from the reference distance, $\Delta(M2-M1)$, is not desirable, but a certain amount of deviation has to be allowed in real structures under the random loadings.

The pointing error due to de-centre of mirror is allowed to a certain extent; when M2 deviates from the reference distance relative to M1 by 1 μm , the angular error is 0.030 arc second (VIS-TRE-01001-9001). Since the allowable error budget is 0.067 arc second, the M2-M1 relative deviation is allowed as

$$\begin{aligned}\Delta(M2-M1) &= \frac{0.067}{0.030} \\ &= 2.233 \mu m\end{aligned}$$

The FEA model computes the displacements of the M2 vertex at the Node 25 and the M1 vertex at the Node 10864. These displacement values are actually the standard deviations (RMS). Therefore, the displacement standard deviation of the difference M2-M1 is not necessarily the difference between the two standard deviations.

In order to calculate the displacement standard deviation of M2 relative to M1, let

m_1 = Random variable representing the M1 vertex displacement

σ_1 = Standard deviation of m_1

m_2 = Random variable representing the M2 vertex displacement

σ_2 = Standard deviation of m_2

σ_{12} = Covariance of m_1 and m_2 .

Then the variance of $m_2 - m_1$ is the expectation of $(m_2 - m_1)^2$

$$\begin{aligned}E[(m_2 - m_1)^2] &= E[(m_2)^2 - 2(m_2)(m_1) + (m_1)^2] \\ &= (\sigma_2)^2 - 2(\sigma_{12}) + (\sigma_1)^2\end{aligned}$$

Therefore the standard deviation of $(m_2 - m_1)$ is

$$\begin{aligned}\sigma(m_2 - m_1) &= \{ E[(m_2 - m_1)^2] \}^{1/2} \\ &= [(\sigma_2)^2 - 2(\sigma_{12}) + (\sigma_1)^2]^{1/2}\end{aligned}$$

This is the displacement standard deviation of the M2 relative to the M1.

The above equations are applied to the three ANSYS models representing the structure with the OSS at the elevation angle of 90°, 50°, and 20°. These models do not contain the soil or the foundation.

A total of 150 modes are extracted using Modal analysis and this resulted in the effective masses listed in Table 2. This model used a 3% damping coefficient

Table 2 – Effective Masses for PSD Analysis

OSS Angle	Direction of Effective Mass		
	X	Y	Z
90°	81.28%	81.09%	80.73%
50°	81.23%	81.59%	82.19%
20°	81.23%	82.58%	81.49%

However, for the Operating Stress case, a wind speed of 11 m/s was applied to the entire structure. The individual wind forces are based on the size and shape of the component exposed to the wind and placed in the model as concentrated loads.

4.4.6 Buffer Impact Loads

The buffer impact load is applied as a torque to the Altitude Axle. The maximum deceleration of the OSS listed in Section 11.1.11 of AD02 is $60^\circ/\text{s}^2$. Using the Mass Moment of Inertia of the OSS about the Altitude Axle, 193,310 $\text{kg}\cdot\text{m}^2$, and the maximum deceleration resulted in a torque of 202,434 N-m. This torque is reacted by beams representing the Buffer and Buffer Strike Plate which tie the OSS to the Yoke. This method applied the correct load to the Altitude Ring, the M1 Cell and the Yoke; however, the M2 may not have been subjected to the load created by the deceleration. The M2 is 3 m away from the Altitude Axis. At a $60^\circ/\text{s}^2$ deceleration, the M2 would see a linear acceleration of 3.2 m/s^2 . Because the MLE loads applied an acceleration of 174 m/s^2 and the structure passed, the M2 can withstand the buffer impact load.

4.4.7 Earthquake Loads

Earthquake loads were originally described in AD08, the Earthquake Analysis Report. Since the earthquake load cases are part of the total mount analysis, this report now includes the descriptions and results.

There are two types of seismic excitations to be applied to the structure. The OBE is an earthquake of moderate size but with a high probability of occurrence during the life time of the observatory, and the MLE is an earthquake of large magnitude but with lower probability of occurrence.

According to Euro-Code 8, the ordinates of response spectrum for the vertical seismic action analysis are modified as follows:

For periods smaller than 0.15 seconds the accelerations are multiplied by 0.7
 For periods greater than 0.50 seconds the accelerations are multiplied by 0.5
 For periods between 0.15 and 0.50 seconds a linear interpolation shall be used

The following tables list the specific OBE 1% and MLE 1% response spectra with the modified vertical responses.

Table 3 – OBE 1% Acceleration Response Spectrum

Frequency [Hz]	Acceleration [m/s ²]	Modified Z [m/s ²]	Frequency [Hz]	Acceleration [m/s ²]	Modified Z [m/s ²]
0.100	2.20036	1.01002	0.833	8.28607	4.14304
0.125	2.34363	1.17182	1.000	9.35492	4.67746
0.167	2.83393	1.41697	1.111	10.04134	5.02067
0.200	3.19676	1.59838	1.250	10.86505	5.43252
0.250	3.71647	1.85824	1.429	11.87507	5.93753
0.333	4.50095	2.25048	1.667	13.15965	6.57983
0.500	5.89341	2.94670	2.500	13.15965	7.23781
0.556	6.32487	3.16234	5.000	13.15965	8.55377
0.625	6.84459	3.42229	10.000	7.75655	5.42958
0.714	7.48198	3.74099	20.000	2.35344	1.64741

Table 4 – MLE 1% Acceleration Response Spectrum

Frequency [Hz]	Acceleration [m/s ²]	Modified Z [m/s ²]	Frequency [Hz]	Acceleration [m/s ²]	Modified Z [m/s ²]
0.100	2.85355	1.42677	0.833	11.73778	5.86889
0.125	3.31443	1.65721	1.000	13.25771	6.62886
0.167	4.01065	2.00533	1.111	14.21870	7.10935
0.200	4.53037	2.26519	1.250	15.38561	7.69281
0.250	5.26582	2.63291	1.429	16.81729	8.40865
0.333	6.37390	3.18695	1.667	18.64121	9.32060
0.500	8.35412	4.17736	2.500	18.64121	10.25266
0.556	8.96268	4.48134	5.000	18.64121	12.11678
0.625	9.68833	4.84416	10.000	10.98272	7.68790
0.714	10.59048	5.29524	20.000	3.33404	2.33383

The two ANSYS models were developed to represent the structure with the OSS at 90° elevation angle and at 0° elevation angle. Both of them contain the foundation and soil

models, and the soil boundary nodes are fixed. A total of 800 modes are extracted. The effective masses are listed in Table 5.

Table 5 – Effective Masses for Response Analysis

OSS Angle	Direction of Effective Mass		
	X	Y	Z
90°	69.83%	69.85%	68.11%
0°	69.83%	68.10%	69.84%

The OBE and MLE acceleration spectra were applied to the soil boundary nodes in X, Y, and Z directions one at a time for a total of six load cases for OBE and six cases for MLE. The SRSS method of mode combination was used with a significant factor above 10^{-7} to recover most of the 800 modes. Then, the output results were obtained in terms of displacements and accelerations

These X, Y, and Z response accelerations were then applied as accelerations onto the Mount model. A set of nodes from the OSS and the Altitude Bearings were averaged to find the overall accelerations of the entire mount. The following table lists these nodes and their locations.

Table 6 – Location of Acceleration Nodes

Component	Node	X (m)	Y (m)	Z (m)
M1 Vertex	2000	0.0	0.0	-0.6894
M1 Centre of Gravity	2100	0.0	0.0	-0.6338
Cassegrain	3000	0.0	0.0	-1.4144
M2 Vertex	4000	0.0	0.0	2.0354
M2 Centre of Gravity	5241	0.0	0.0	2.6022
Inner Elev. Bearing +X	4301	3.1542	0.0	0.0
Outer Elev. Bearing +X	110470	3.2524	0.0	0.0
Inner Elev. Bearing -X	4302	-3.1542	0.0	0.0
Outer Elev. Bearing -X	101292	-3.2524	0.0	0.0

The average accelerations of these nodes from the MLE analysis resulted in the accelerations in Table 7.

Table 7 –MLE Acceleration Results

OSS at 94 deg	a_x	a_y	a_z
X Response	14.8328	2.5509	6.2615
Y Response	1.8828	11.1189	2.6602
Z Response	2.9653	4.5165	5.3150
<i>SRSS Acceleration</i>	<i>16.3011</i>	<i>11.5867</i>	<i>7.5790</i>

OSS at -4 deg	a_x	a_y	a_z
X Response	14.7366	6.4485	4.2873
Y Response	2.6785	5.9949	2.8086
Z Response	2.3678	4.5075	11.5372
<i>SRSS Acceleration</i>	<i>16.6472</i>	<i>7.1415</i>	<i>12.6107</i>

The SRSS Accelerations are the square root of the sum of the squared accelerations from the X response, the Y response and the Z response. Section 14.1.1.5 of AD02 states that the accelerations from a single response case must be combined by SRSS.

Section 3.3.5.2 (4) of Part 2 of AD15 states that these resulting accelerations are combined in the following manner:

$$\begin{aligned}
 \text{Load 1:} & \quad (1.0 * a_x) + (0.3 * a_y) + (0.3 * a_z) \\
 \text{Load 2:} & \quad (0.3 * a_x) + (1.0 * a_y) + (0.3 * a_z) \\
 \text{Load 2:} & \quad (0.3 * a_x) + (0.3 * a_y) + (1.0 * a_z)
 \end{aligned}$$

Applying the MLE accelerations to the previous equations and adding the acceleration of gravity result in the following accelerations applied to the mount model.

Table 8 –MLE Acceleration Inputs to FEA

OSS at 94 deg	a_x	a_y	a_z
Load Case 1	16.3011	4.1601	12.0564
Load Case 2	4.8903	12.2707	12.0564
Load Case 3	4.8903	4.1601	17.3617

OSS at -4 deg	a_x	a_y	a_z
Load Case 1	16.6472	11.9251	4.4673
Load Case 2	4.9942	16.9242	4.4673
Load Case 3	4.9942	11.9251	13.2948

These loads were not used to determine the Azimuth Bearing Loads nor the Foundation Interface Loads, instead, these component loads came from the response spectrum FEA.

4.4.8 M1 Cell Loads

The loads for the M1 cell were derived to account for the action of the pneumatic actuators. Their derivation is described in detail in AD07.

4.4.9 Component Loads

To find the loads on the individual components and interfaces, the accelerations in Table 8 were not used. Instead the accelerations at the locations being analysed were used. Table 9 through 12 contain these accelerations.

Table 9 –MLE Acceleration Inputs for M1 Cell

OSS at 94 deg	a_x	a_y	a_z
Load Case 1	11.9536	4.1616	12.0208
Load Case 2	3.5861	12.2759	12.0208
Load Case 3	3.5861	4.1616	17.2431

OSS at -4 deg	a_x	a_y	a_z
Load Case 1	13.9804	11.4073	4.5405
Load Case 2	4.1941	15.1982	4.5405
Load Case 3	4.1941	11.4073	13.5387

Table 10 –MLE Acceleration Inputs for M2

OSS at 94 deg	ax	ay	az
Load Case 1	23.9359	4.5632	12.1585
Load Case 2	7.1808	13.6145	12.1585
Load Case 3	7.1808	4.5632	17.7020

OSS at -4 deg	ax	ay	az
Load Case 1	20.0463	12.2037	5.5341
Load Case 2	6.0139	17.8528	5.5341
Load Case 3	6.0139	12.2037	16.8509

Table 11 –MLE Acceleration Inputs for Cassegrain

OSS at 94 deg	ax	ay	az
Load Case 1	11.7935	4.9426	11.7644
Load Case 2	3.5381	14.8792	11.7644
Load Case 3	3.5381	4.9426	16.3884

OSS at -4 deg	ax	ay	az
Load Case 1	14.4750	11.5107	4.7689
Load Case 2	4.3425	15.5429	4.7689
Load Case 3	4.3425	11.5107	14.3001

Table 12 –MLE Acceleration Inputs for Altitude Bearings

OSS at 94 deg	ax	ay	az
Load Case 1	16.3011	4.1601	12.0564
Load Case 2	4.8903	12.2707	12.0564
Load Case 3	4.8903	4.1601	17.3617

OSS at -4 deg	ax	ay	az
Load Case 1	16.6472	11.9251	4.4673
Load Case 2	4.9942	16.9242	4.4673
Load Case 3	4.9942	11.9251	13.2948

4.5 FEA Results

4.5.1 FEA Results Summary

Table 13 summarizes the specification requirements and the analysis results.

Table 13 - Summary of Results

Item	Spec Section	Spec Value	Actual Value	Report Section	Comments
1 st Locked Rotor Frequency	8.6.1.2	11.4 Hz	11.31 Hz	4.5.2	
Element Mesh Errors	14.1.1	≤ 10%	47.4%	4.5.4	See Note 1
Operating: Max stress	14.1.3	118 MPa	44.4 MPa	4.5.5	Max stress over load combinations A-E
Short Term Accidental: Max Stress	14.1.3	237 MPa	235.3 MPA	4.5.6	See Note 2
Survival: Max Stress	14.1.3	296 MPa	235.3 MPa	4.5.6	See Note 3
Platform Motion	RID 175	5 mm	2.03 mm	4.5.7	

Note 1: Of the 101,196 elements in the Vista Mount Model, 10 had element mesh errors over 10%: the two highest elements are 47% and 45%, the other eight are between 15% and 11% and the remaining elements are below 10%. These elements are all in a low stress area of the Yoke and the displacements are not important.

Note 2: Of the 101,828 nodes in the Vista Mount Model, 4 nodes exceeded the allowable stress of 237 MPa. Load Case 2 at 94° had three nodes above the allowable and Load Case 1 at -4° had only one node above the limit. These nodes are anomalies within the model. Artificially stiff beams were used to connect various components together. This modeling method produced the required load transfer between components and reduced the number of DOF, but it produced unrealistic loads because the force is transferred through a single point. These 4 nodes are results of these point loads.

Note 3: Of the 101,828 nodes in the Vista Mount Model, 1 node exceeded the allowable in Load Case 2 at 94°. This particular area has the same modeling anomaly as discussed in Note 2.

4.5.2 Locked Rotor Frequency

The locked rotor frequencies were determined according to Section 8.6.1.1 of AD02, and are given in Table 14. Section 4.2.3 explains the methods used to find the LRR for this model. The altitude locked rotor frequency is given in Figure 16. The azimuth locked rotor frequency is given in Figure 17 and the M2 frequency is shown in Figure 18.

Table 14 - First Natural Frequencies of Mount

Frequency [Hz]	Description
9.20	A sidesway mode, where the structure oscillates in the plane of the altitude axis.
11.31	The altitude LRR mode. The OSS is decoupled from the yoke and simply translates back and forth while the yoke oscillates as a cantilever.
11.55	The azimuth LRR mode. The azimuth rotating structure oscillates about the azimuth axis.
20.06	The M2 instrument oscillates about the optical axis.

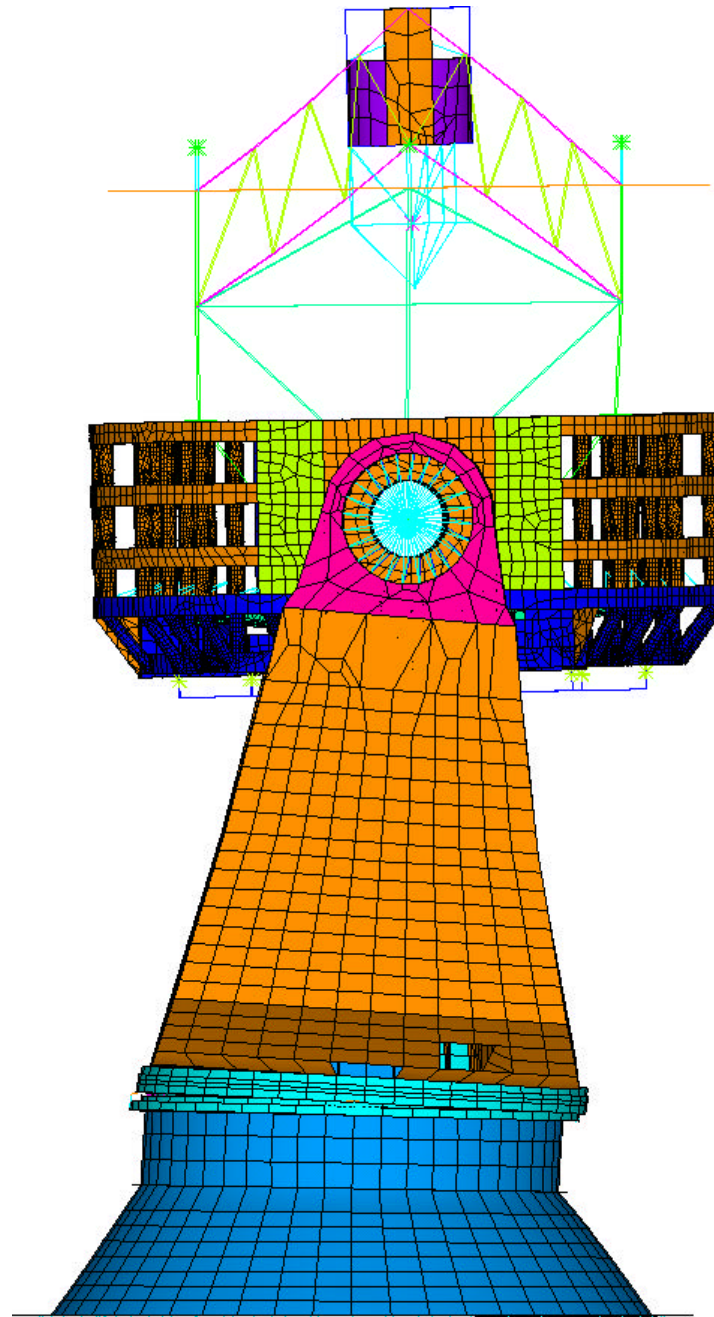


Figure 16 - Altitude Locked Rotor Resonance

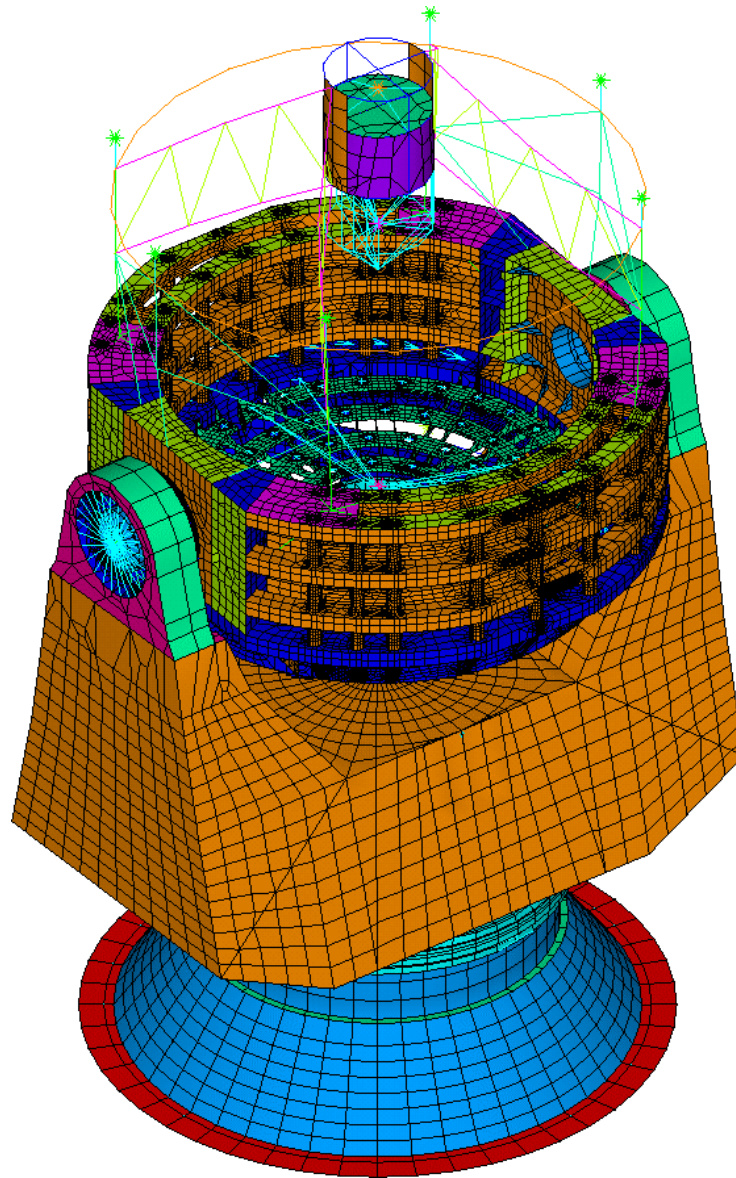


Figure 17 - Azimuth Locked Rotor Resonance

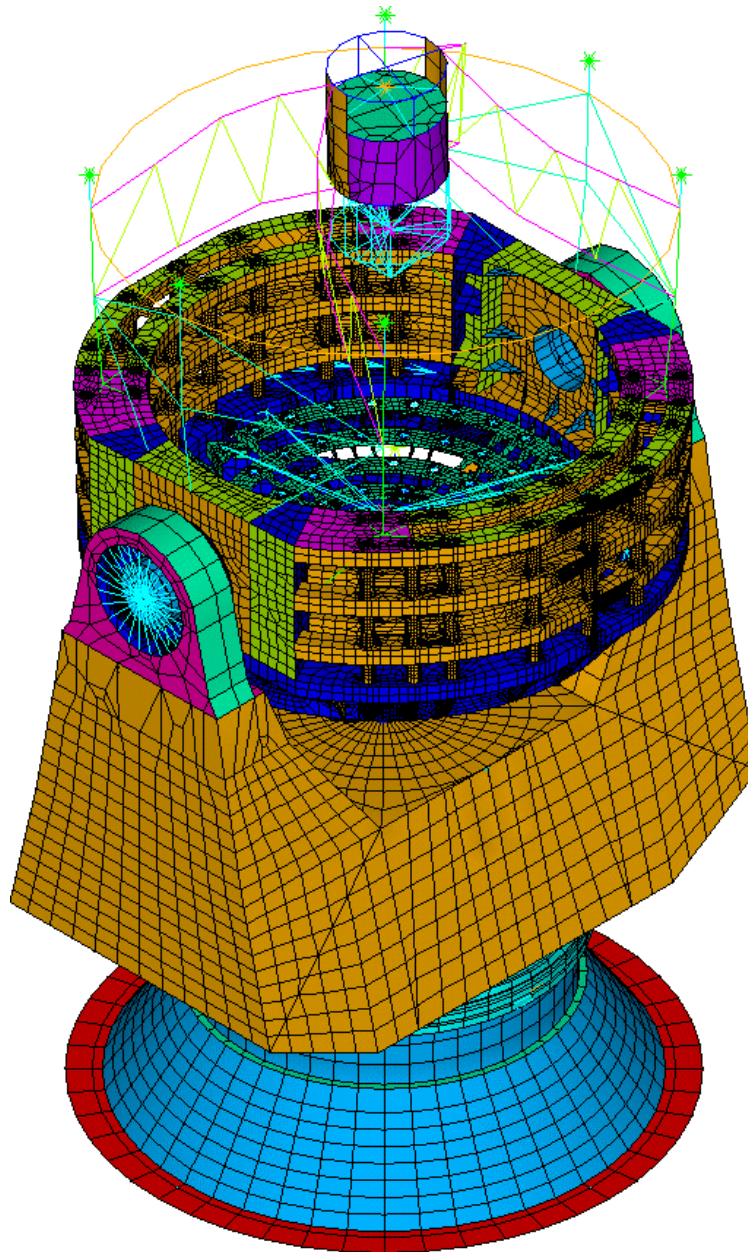


Figure 18 – M2 Locked Rotor Resonance

4.5.3 Mesh Density Error

The mesh density error for the mount is shown in Figure 19. As the figure shows, the vast majority of the mesh is below 10%, but there are 10 elements above 10%.

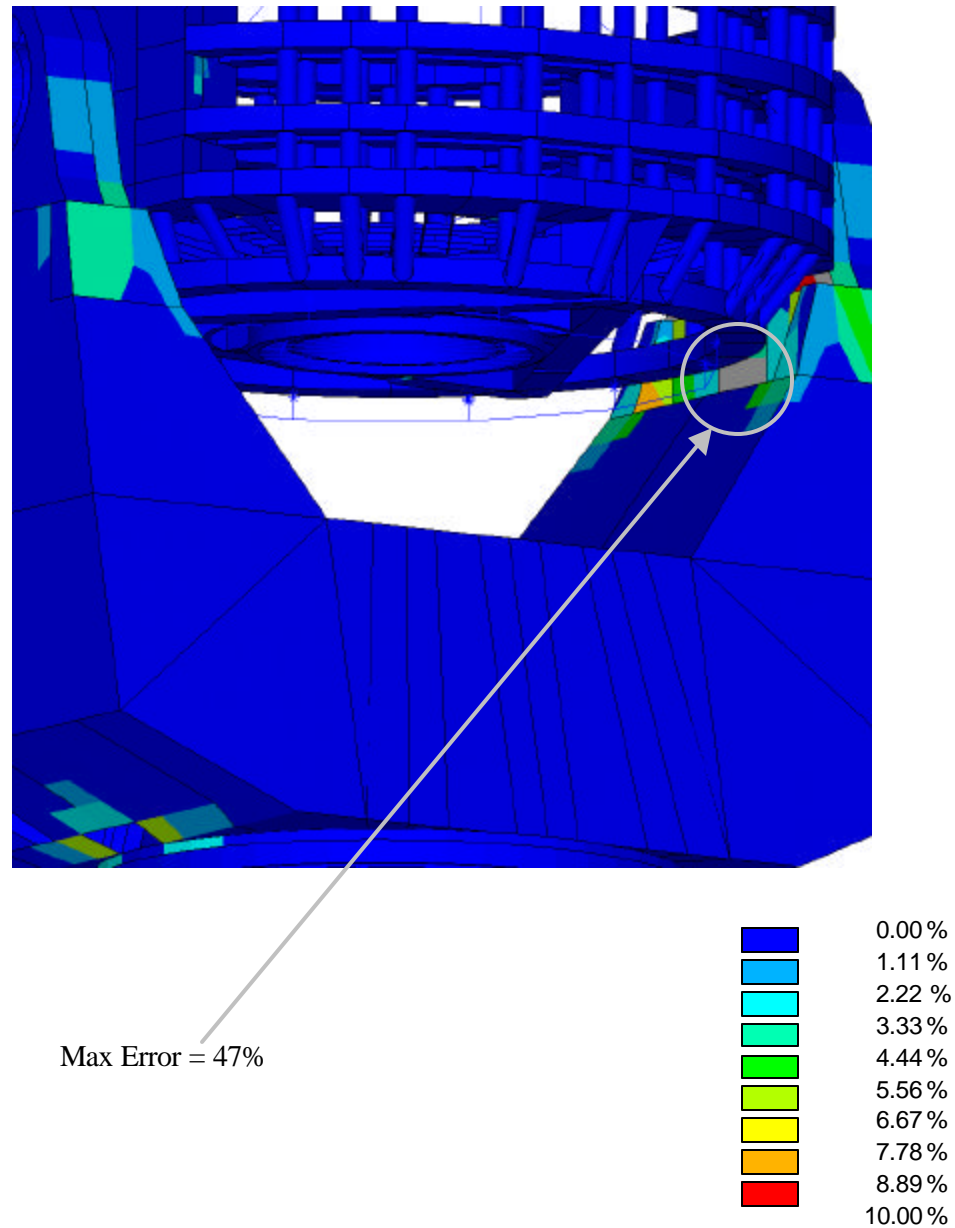


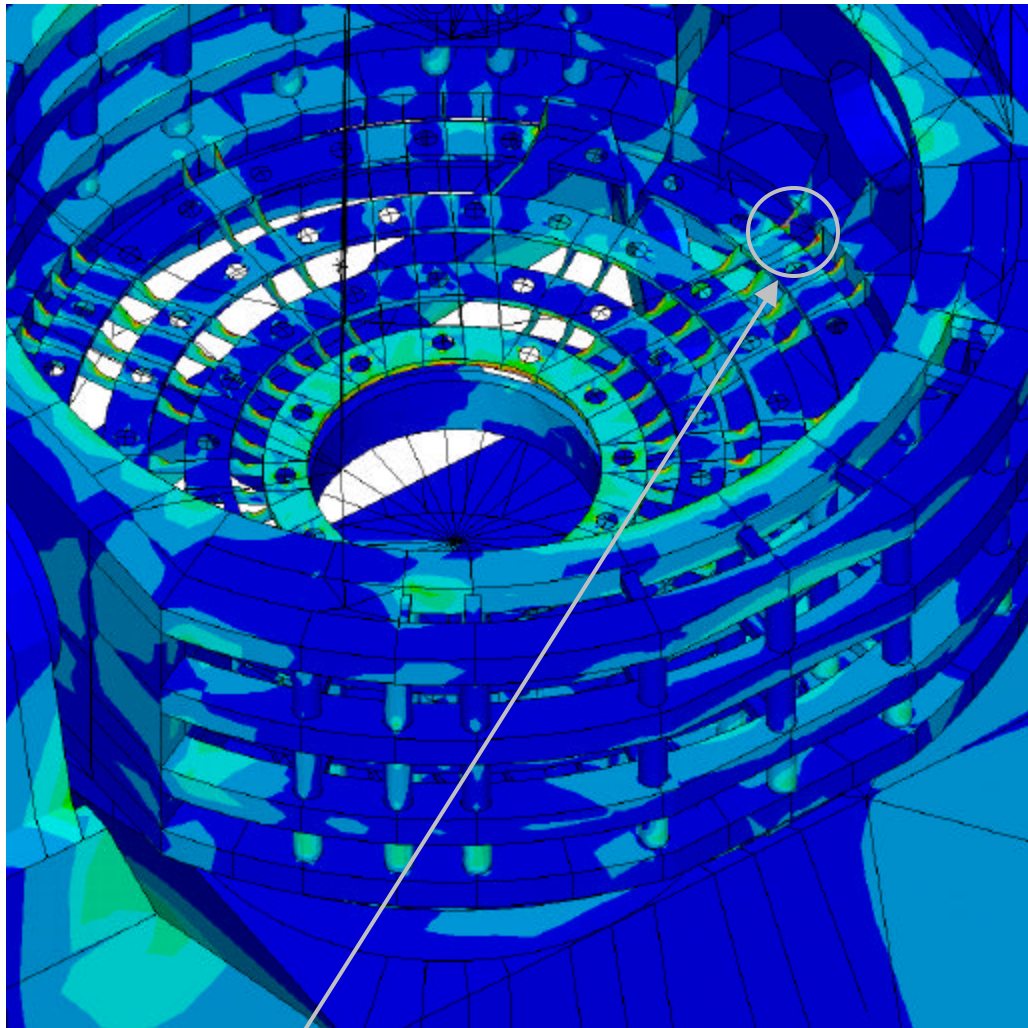
Figure 19 - Mesh Density Error for Mount FEA Model

4.5.4 Operating Load Cases, Maximum Stress

Operating load cases comprise load combinations A-E in Table 1. These load combinations were identified as operating load cases in the specification. Results for each load combination are shown in Table 15. The stress plots for each load combination are listed in Figures 20 through 24.

Table 15 - Results for Operating Load Cases

Load Combination	Maximum Stress [MPa]	Allowable Stress [MPa]	Location
A	44.5	118	Mirror Basket Connection
B	23.0	118	Centre Cone
C	34.6	118	Mirror Basket Connection
D	26.0	118	Centre Cone
E	44.5	118	Mirror Basket Connection



Max Stress = 44.5 MPa

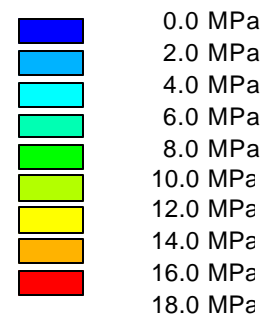
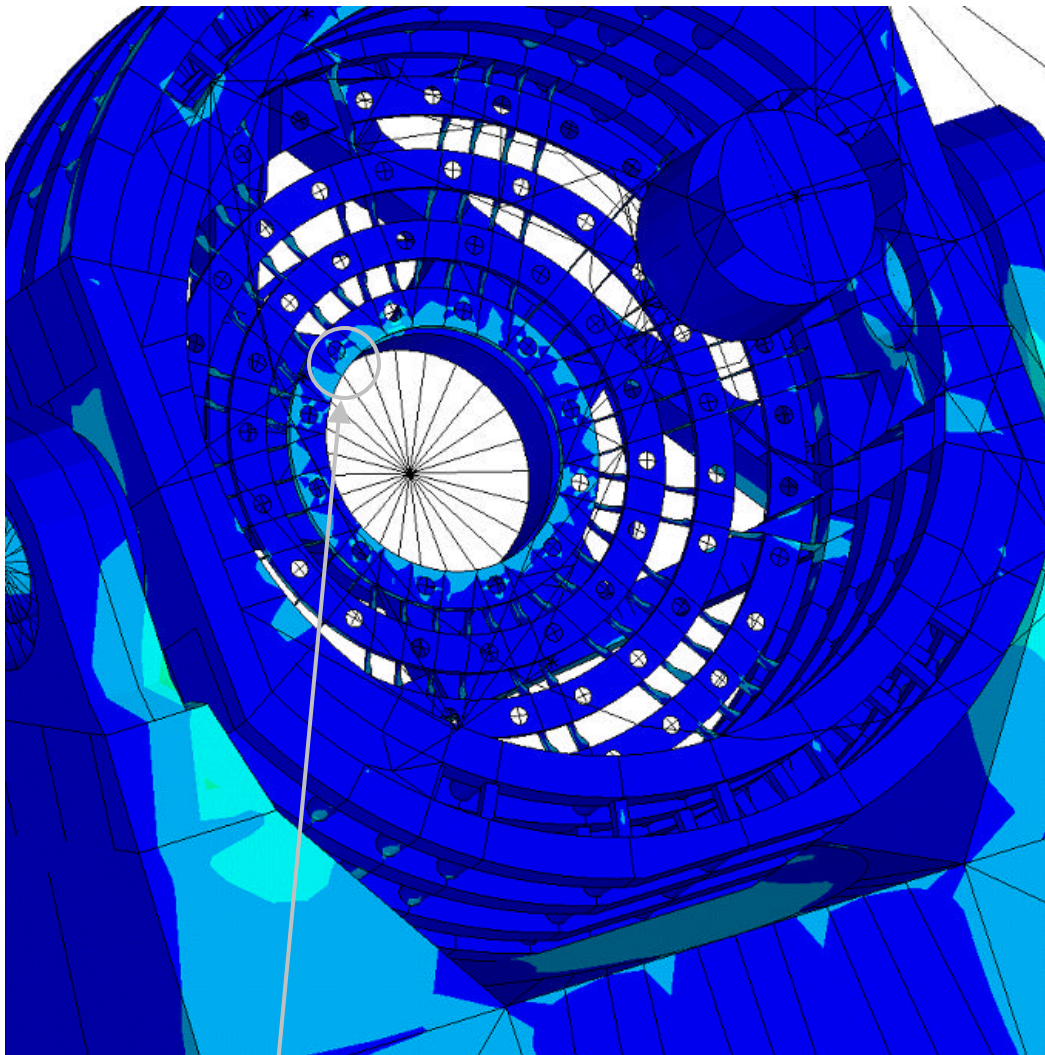


Figure 20 - Stress Plot for Load Combination A



Max Stress = 23.0 MPa

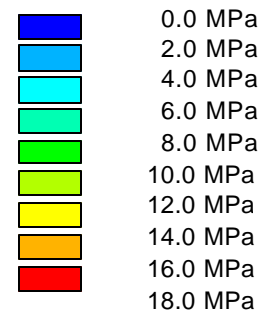
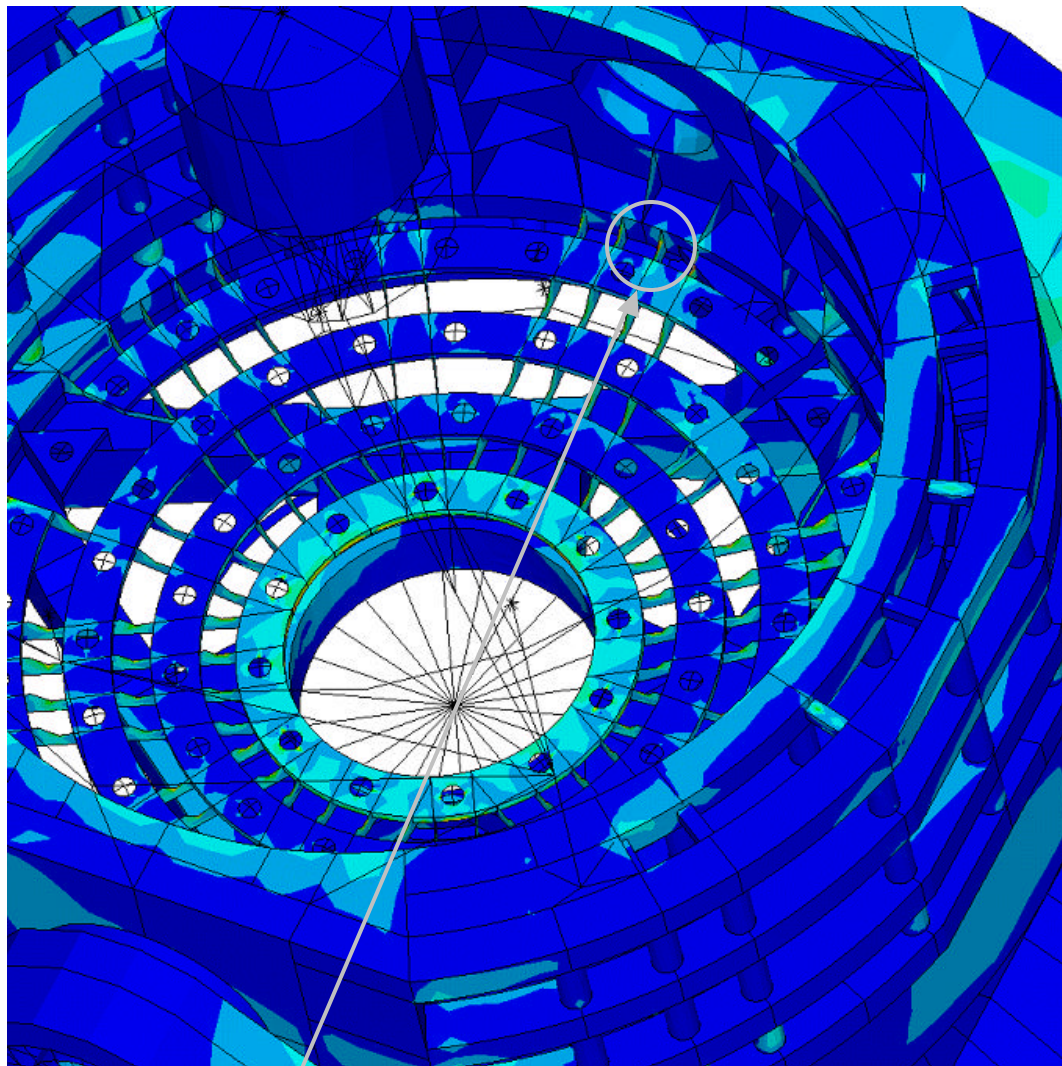


Figure 21 - Stress Plot for Load Combination B



Max Stress = 34.6 MPa

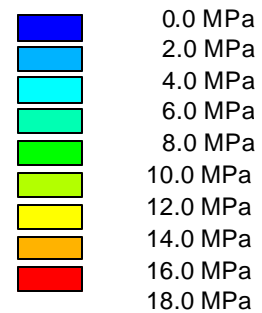
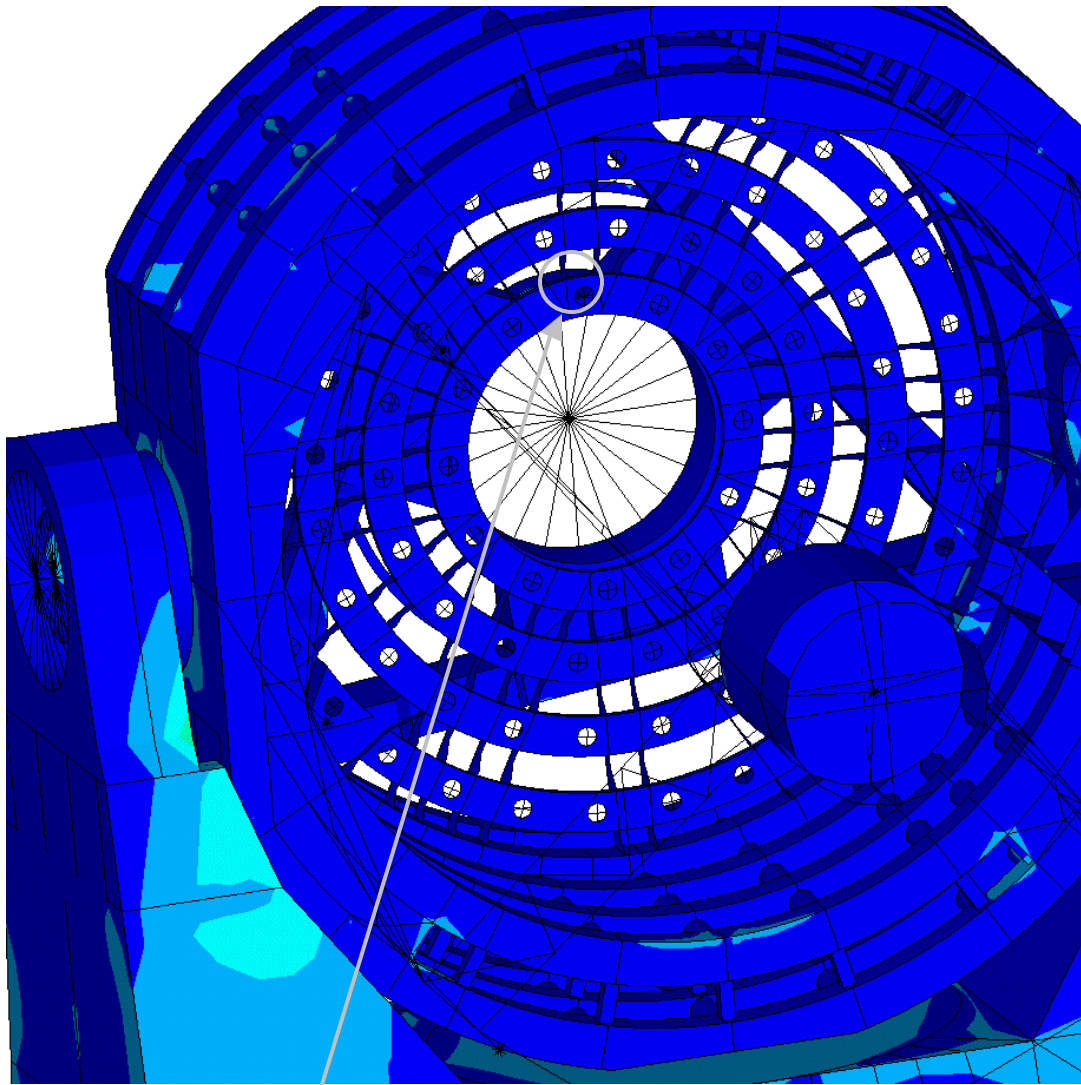


Figure 22 - Stress Plot for Load Combination C



Max Stress = 26.0 MPa

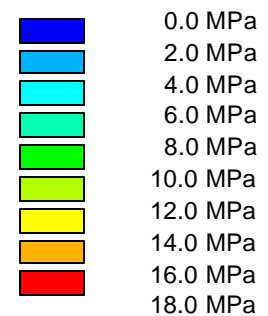
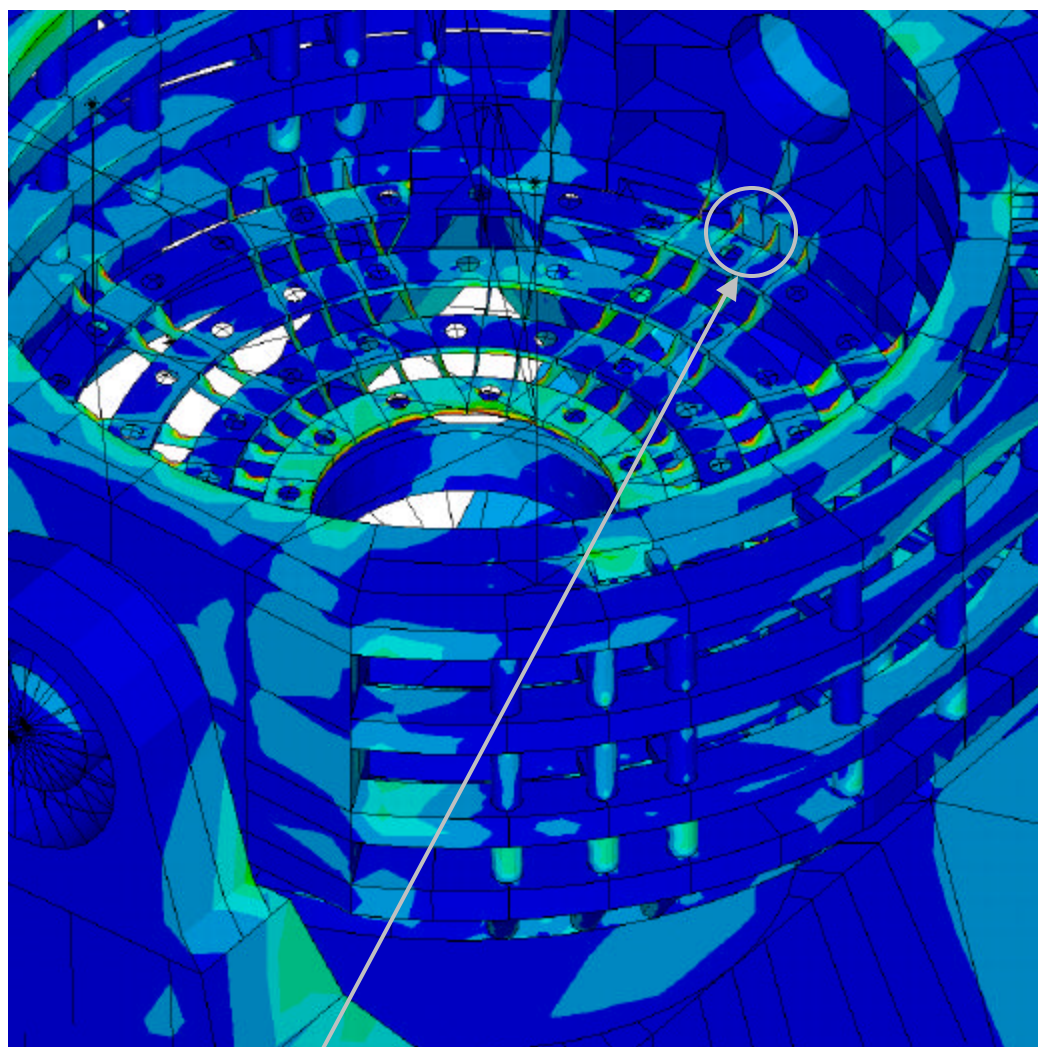


Figure 23 - Stress Plot for Load Combination D



Max Stress = 44.5 MPa

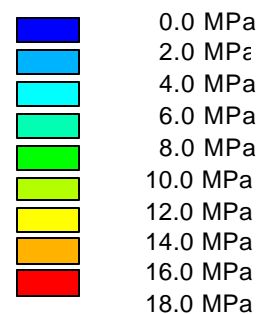


Figure 24 - Stress Plot for Load Combination E

4.5.5 Survival / Accidental Load Cases, Maximum Stress

The short term accidental load cases and the survival load cases were combined into a single set of loads. These loads include three different MLE accelerations, Survival Winds, maximum thermal change and the buffer load. The mount can return to service after being subjected to these loads. The results for each load combination are given in Table 16. Stress plots for each load combination are given in Figures 25 - 30. Of the six different loadings, two cases showed nodes above the allowable of 237 MPa. One load case had three nodes above the allowable and the other only had one node above the allowable. As stated in Section 4.5.1 the high stresses are anomalies from a modelling technique.

Table 16 - Results for Short Term Accidental Load Cases

Load Combination	Maximum Stress [MPa]	Allowable Stress [MPa]	Location
1 - 1	201.6	237	Buffer Attachment
1 - 2	235.3	237	Buffer Attachment
1 - 3	< 100.0	237	M1 Cell
2 - 1	235.3	237	Top of Altitude Ring
2 - 2	138.4	237	Top of Altitude Ring
2 - 3	142.9	237	Top of Altitude Ring

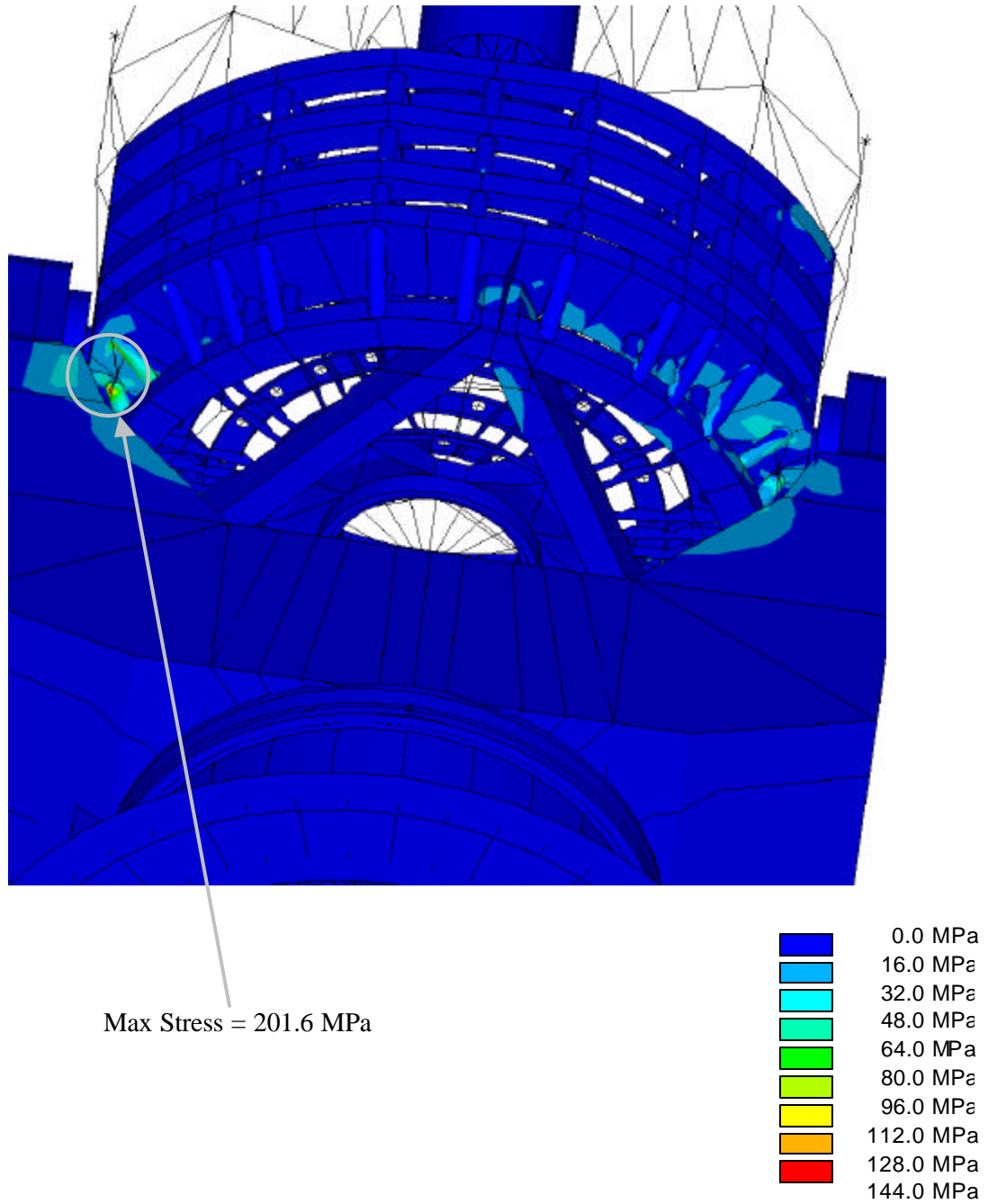


Figure 25 - Stress Plot for Load Combination 1 - 1

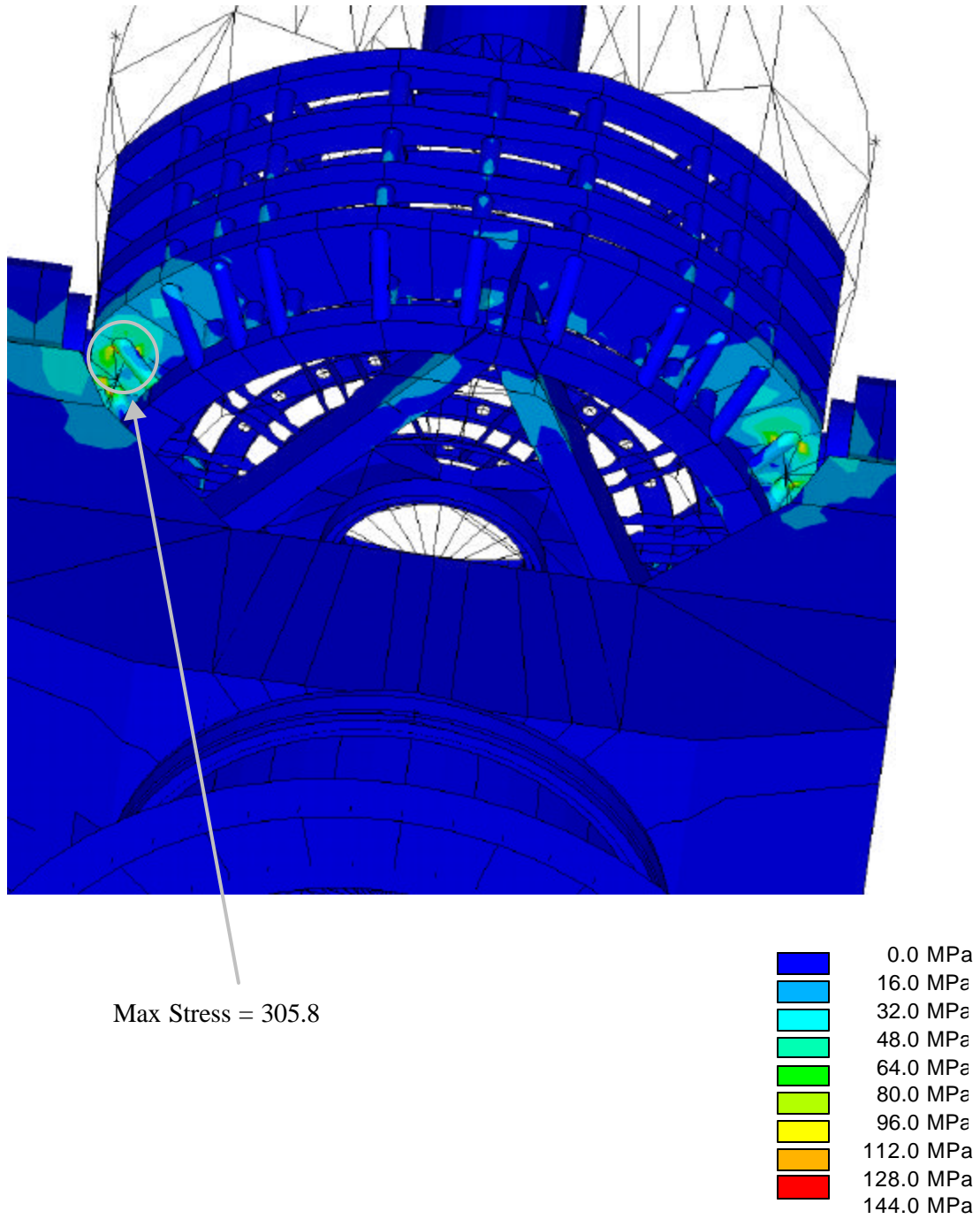
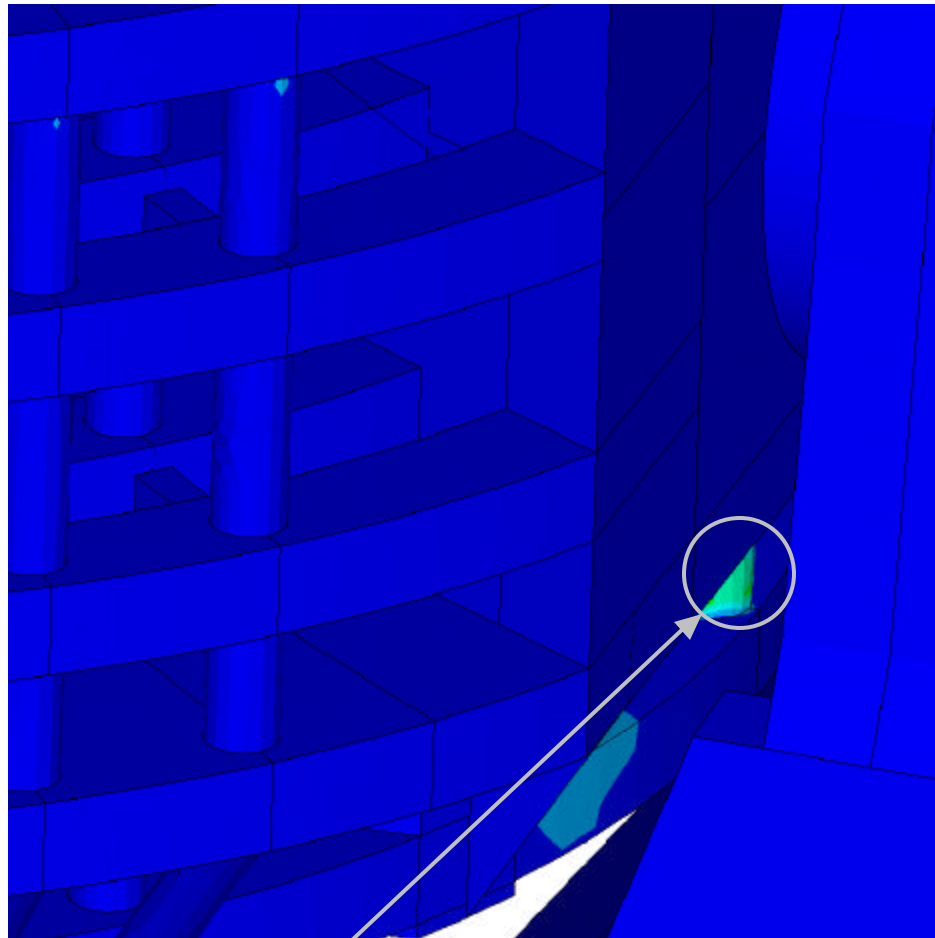


Figure 26 – Stress Plot for Load Combination 1 - 2



Max Stress = 100 MPa

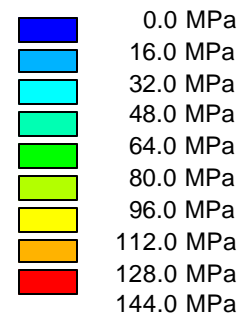
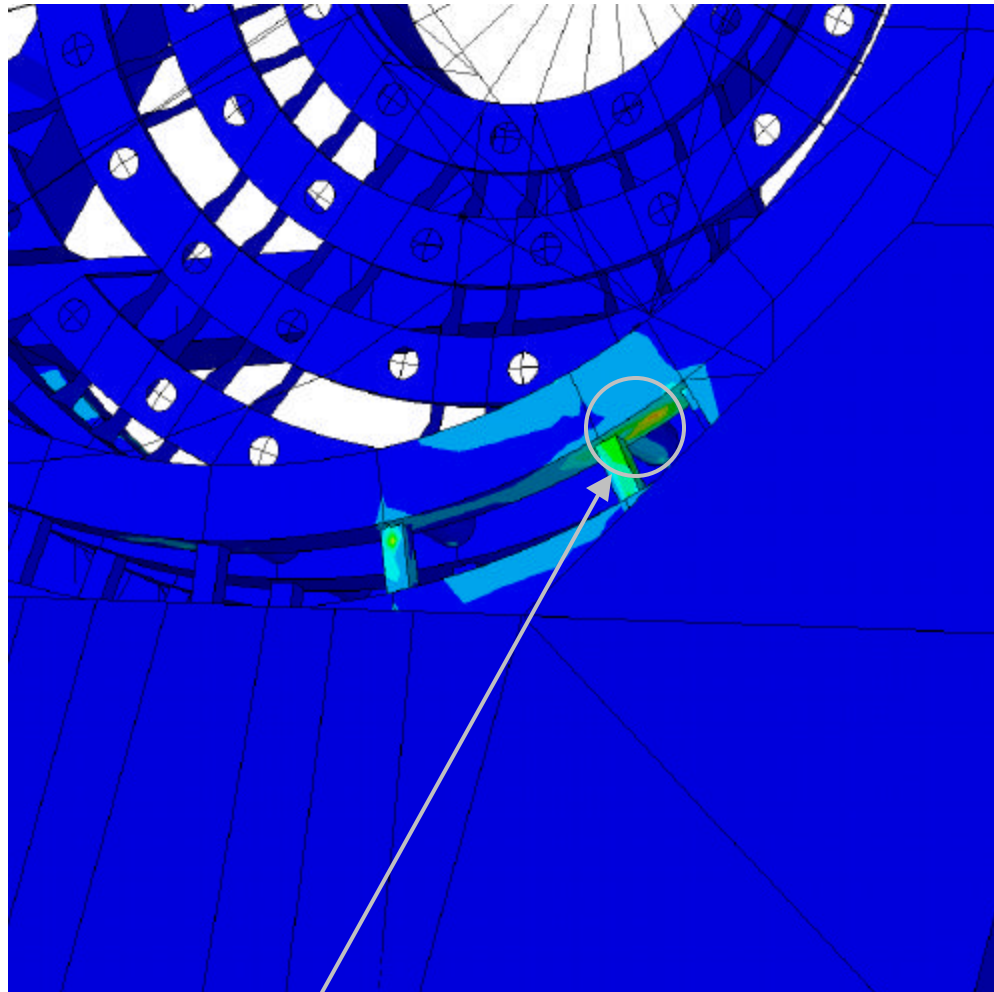


Figure 27 - Stress Plot for Load Combination 1 - 3



Max Stress = 243.4 MPa

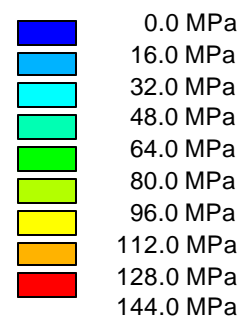
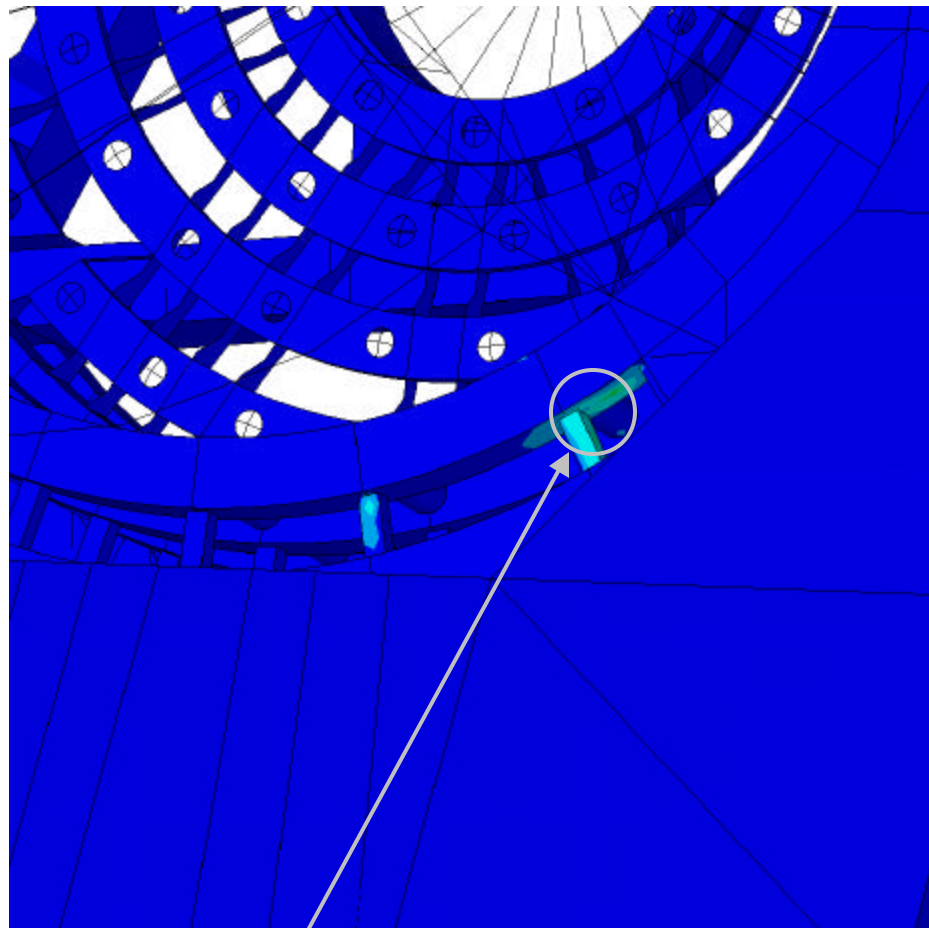


Figure 28 - Stress Plot for Load Combination 2 - 1



Max Stress = 138.4 MPa

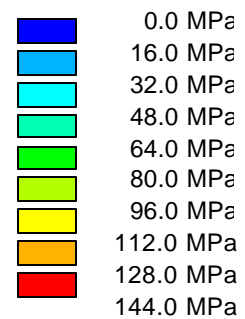
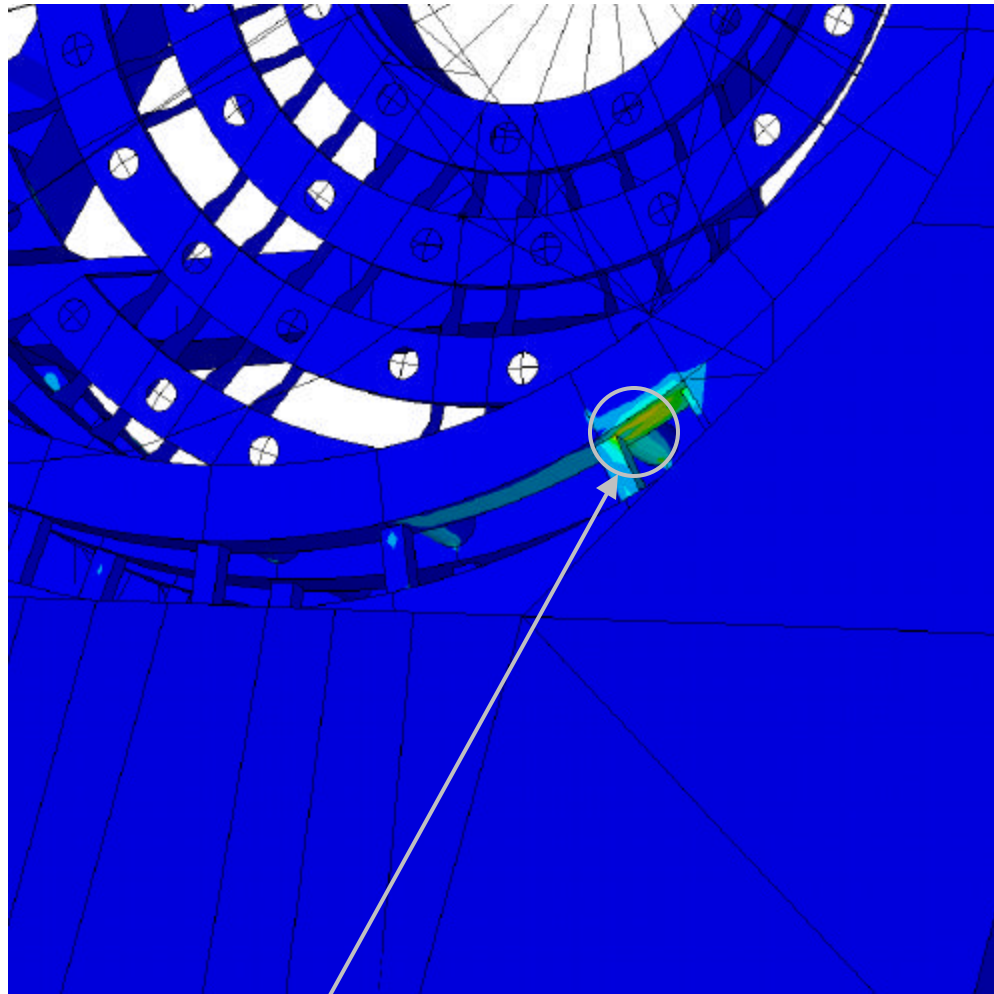


Figure 29 - Stress Plot for Load Combination 2 - 2



Max Shear = 142.9 MPa

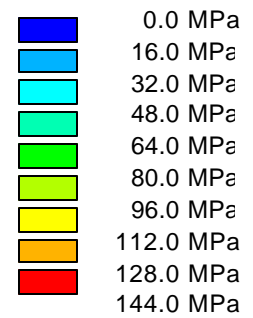


Figure 30 - Stress Plot for Load Combination 2 – 3

4.5.6 Platform Motion

In response to RID 175, the platform motion was measured under 1% MLE to determine if the platform would close the 5 mm gap to the floor. Table 17 shows that the platform does not move enough to contact the floor. Figure 31 shows the location of the platform.

Table 17 - Results Platform Motion

Direction	Distance [mm]	Allowable [mm]
X Motion	1.69	5
Y Motion	1.12	5
SRSS	2.03	5

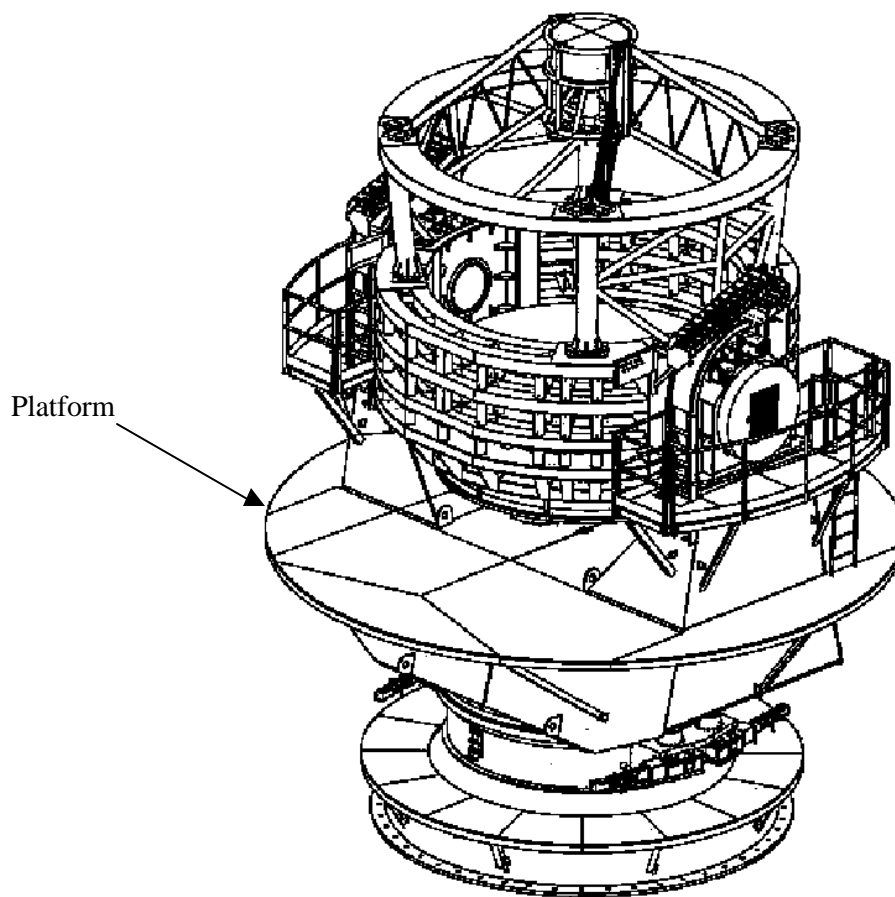


Figure 31 – Platform Location

4.5.7 M1 to M2 Motion from Wind

The following steps produced the results in this section. Section 4.4.5 discusses these steps in more detail.

1. Input Karman velocity PSD is applied.
2. Compute the wind forces on the structure including the exposed areas, drag coefficients, attenuating factors on the secondary structural members.
3. Combine 150 modes.
4. Compute Participating Factors.
5. Compute covariance between the M1 and M2 RMS displacements.
6. Compute the statistical difference between M1 and M2 displacements.

The local coordinate system is listed below and remains fixed.

X = parallel to the El Axle
Y = perpendicular to El Axis and parallel to the M1 mirror
Z = perpendicular to the M1 mirror.

The displacements listed as 0.0 are negligible.

Table 18 - M1 – M2 Maximum Displacements

OSS Angle	Wind Direction	DX [mm]	DY [mm]	DZ [mm]
90 deg	X Wind	2.447	0.000	0.000
	Y Wind	0.000	3.489	0.000
50 deg	X Wind	2.138	0.000	0.000
	Y Wind	0.000	2.810	0.546
20 deg	X Wind	1.722	0.000	0.000
	Y Wind	0.000	2.806	0.660

Table 19 - M1 – M2 Correlated Displacements

OSS Angle	Wind Direction	DX [mm]	DY [mm]	DZ [mm]
90 deg	X Wind	2.366	0.000	0.000
	Y Wind	0.000	1.317	0.000
50 deg	X Wind	2.078	0.000	0.000
	Y Wind	0.000	0.331	0.189
20 deg	X Wind	1.676	0.000	0.000
	Y Wind	0.000	0.889	0.254

4.6 Component Results

4.6.1 Cassegrain Bearing

The Cassegrain rotator bearing loads were derived using the seismic accelerations listed in Section 4.4.7. The accelerations were combined using the method described in that section. The acceleration load cases used are given in Table 20. These accelerations do not include the dead weight of the bearing or Cassegrain instrument, which was added separately.

Table 20 – Cassegrain Accelerations

	Max Horizontal Acceleration		Max Vertical Acceleration	
	G _{horizontal} [g]	G _{vertical} [g]	G _{horizontal} [g]	G _{vertical} [g]
OBE	1.039	.167	.414	.558
MLE	1.472	.237	.586	.791

The bearing capacity is measured by using an equivalent thrust load. The bearing vendor has provided an equation that allows the thrust, radial, and overturning loads to be combined into a single load. The bearing was checked for the OSS pointing to horizon and zenith. At horizon, the weight of the Cassegrain instrument puts a radial load on the bearing, while at zenith the load is axial. The largest bearing load occurs for the MLE case, at horizon pointing, at the maximum vertical acceleration. This makes sense, considering that the largest vertical acceleration would put the largest radial and moment loads on the bearing at horizon. The dead weight of the Cassegrain instrument was considered in the calculation. Table 21 summarizes the results.

Table 21 – Cassegrain Bearing Results

Maximum Equivalent Thrust Load [N]	Bearing Capacity [N]	Factor of Safety
278,096	901,208	3.2

4.6.2 Altitude Bearings

The altitude bearing loads were derived using the seismic accelerations listed in Section 4.7.7. The accelerations were combined using the method described in that section. The acceleration load cases are given in the table below. We ran the calculation for MLE loads first, compared them to OBE allowables and found the bearings to have factors of safety greater than one. Therefore the OBE loads were not applied. The thrust acceleration acts down the altitude axis of the telescope, putting a thrust load on the bearings. The radial acceleration is a vector combination of vertical and horizontal accelerations that load the bearings radially. The numbers listed in the table include gravity.

Table 22 – Altitude Bearing Input Loads

MLE Loads	G_{thrust}	G_{radial}
Max Thrust Acceleration [m/sec ²]	14.08	6.00
Max Radial Acceleration [m/sec ²]	4.22	13.15
Transposing Thrust Acceleration [m/sec ²]	6.00	14.08

The altitude bearings were assumed to resist a mass equal to the effective mass for the sidesway mode of the telescope. This mass was 76,537 kg, 1.53 times the OSS mass of 49,880 kg. This was a conservative assumption to account for any contribution the mass of the yoke could possibly make to the bearing load during an earthquake. It was further assumed that only two bearings took the thrust load, one on each axle.

The factors of safety are shown below. The bearings factor of safety is measured against an equivalent radial load, the formula being provided by the manufacturer. The equivalent radial load is then divided into 50% of the static load rating of the bearing. Using 50% of the static load rating is recommended for slow moving applications and would qualify as an OBE allowable. We used the smallest static load rating for the two bearings.

Table 23 – Altitude Bearing Results

Load Case	Thrust Load [N]	Radial Load [N]	Equiv. Radial Load [N]	Factor of Safety
Max Thrust Acceleration	538,850	114,759	935,057	1.72
Max Radial Acceleration	161,655	251,617	469,472	3.43
Transposing Thrust Acceleration	229,518	269,425	590,152	2.72

4.6.3 Foundation Interface

The foundation loads are given in Table 24. These loads were derived using the response spectrum, combining modes with the SRSS method. These loads were combined as in previous issues of this report. For each mode, we find net forces and moments for the bolt pattern in each coordinate direction. These forces and moments are then combined using the SRSS method. After the SRSS combination of the modal results, the shears and moments from the different coordinate directions are combined to produce a net horizontal shear and overturning moment. The largest loads come from the MLE seismic case, which should be the design case. The largest torsional loads on the anchor bolts come when the OSS is oriented at horizon. The large mass of the M2 creates a larger azimuth moment at that orientation.

Table 24 – Foundation Results

	Shear [kN]	Axial [kN]	Overturning [kN-m]	Torsion [kN-m]
Max Shear and Overturning Moment	952	1240	6753	76.5
Max Axial Load and Torsion	379	1400	2575	255


4.6.4 Azimuth Bearing

The azimuth bearing is analysed in a separate report.

4.6.5 Component Interfaces

The bolted interfaces between the Cassegrain Instrument and the bearing, the M2 Instrument to the M2 Frame, M2 Structure to the Altitude Ring, M1 Cell to Altitude Ring, and the Altitude Bearing Housing to the Yoke are contained within the Appendix. All these components used the accelerations from the MLE analysis.

5 Appendix

	SYSTEM:	Vista	NAME:	Adkins
	DRAWING NUMBER:		DATE:	24 May 04
TOPIC: Connection Analysis Overview			PROJECT:	
			PAGE:	1

The following analyses determine if the bolts attaching various components can withstand the given forces.

All of the analyses follow the same procedure:

After determine the bolt force through basic statics, the analyst used the following bolt equation from:

MIL-HNBK-5E & Machine Design by Deutschman

$$F_{Ten} = \text{Preload} + (0.3)(F_{ext})$$


where

$$\text{Preload} = \text{Allowable Tension} \cdot 0.75$$

$$F_{ext} = \text{Applied Force}$$

Then the following Interaction Equation determined if the bolt passed

$$\left(\frac{F_{Ten}}{F_{allow Ten}} \right)^2 + \left(\frac{F_{shear}}{F_{allow shear}} \right)^2 \leq 1$$

 <p>Vertex RSI A TriPoint Global Company</p>	SYSTEM:	Vista	NAME:	Adkins
	DRAWING NUMBER:		DATE:	29 May 04
TOPIC: Connection Analysis Overview			PROJECT:	
			PAGE:	2

The allowables for the bolts themselves are as follows:

Use 10.9 Bolts $Ten = 1040 \text{ MPa}$
 $Shear = 600 \text{ MPa}$

Dia	Area	Preload	Ten	Shear
12 mm	84.3 mm ²	65,800 N	87,700 N	50,600 N
16 mm	157 mm ²	122,500 N	163,300 N	94,200 N
20 mm	245 mm ²	191,100 N	254,800 N	147,000 N
30 mm	561 mm ²	437,600 N	583,400 N	336,000 N



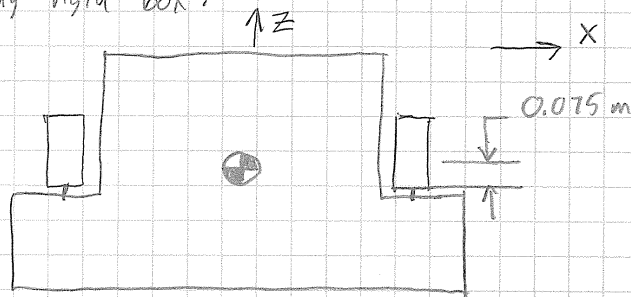
SYSTEM: Vista
DRAWING NUMBER:

NAME: Adkins
DATE: 24 May 04
PROJECT:
PAGE: 1

TOPIC: Cassegrain Instrument Attachment

Determine the Bolt Forces and Interactions
between the Cassegrain Instrument and the Cass Bearing.

Assume the Cassegrain Instrument acts as the
following rigid box:



$$\text{Mass} = 2,900 \text{ Kg}$$

Cassegrain Accelerations @ MLE @ 94°

$$X = 11.8 \text{ m/s}^2 \quad Y = 14.9 \text{ m/s}^2 \quad Z = 16.4 \text{ m/s}^2$$

Find Bolt Shear Force


$$\text{Shear Force} = M * a$$

$$F = 2900(\sqrt{11.8^2 + 14.9^2})$$

$$F = 55,119 \text{ N}$$

per bolt

$$F = 55,119 / 36 = \underline{1,531 \text{ N}}$$

	SYSTEM:	Vista	NAME:	Adkins
	DRAWING NUMBER:		DATE:	24 May 04
TOPIC: Cassegrain Instrument Attachment			PROJECT:	
			PAGE:	2

$$\text{Axial Force} = M \times d$$

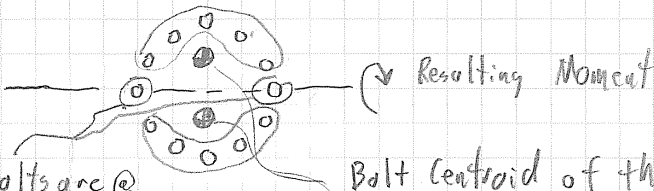
$$F = 2,900 \times 16.4$$

$$F = 47,560 \text{ N/4 Bolts}$$

$$F = \underline{1,321 \text{ N}}$$

To find the axial force due to the overturning moment, use the following method:

For a circular bolt pattern, assume the reacting forces occur at the bolt centroid.



These bolts are @ the pivot so they are not used in this method

Finally use the distance between the centroids as the reactions.

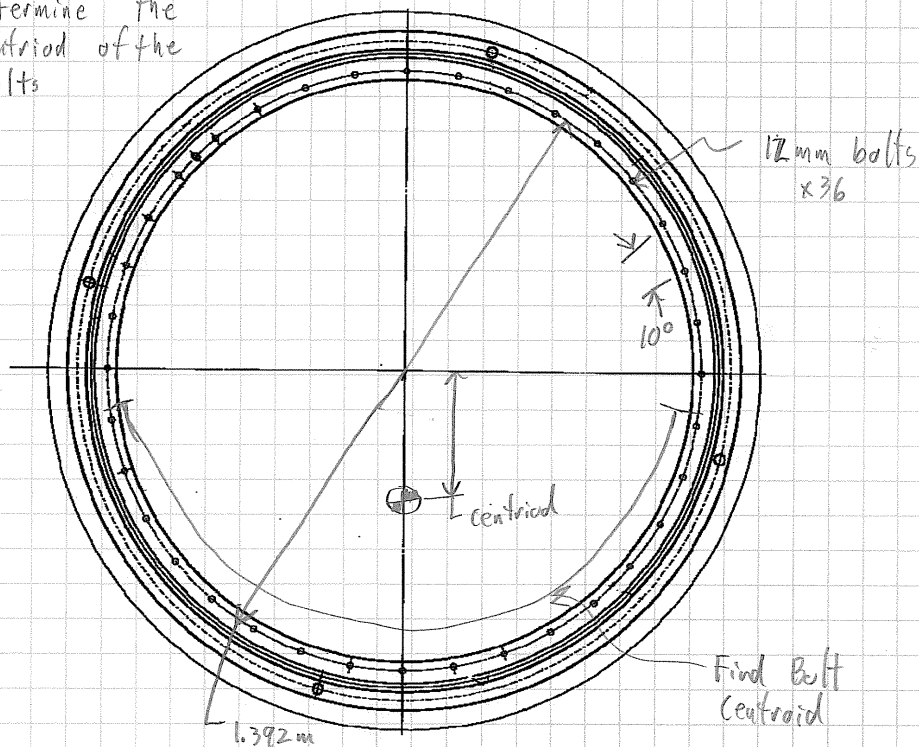


SYSTEM:
Vista
DRAWING NUMBER:

NAME: *Adkins*
DATE: *24 May 04*
PROJECT:
PAGE: *3*

TOPIC: *Cassegrain Instrument Attachment*


Determine the
Centroid of the
Bolts



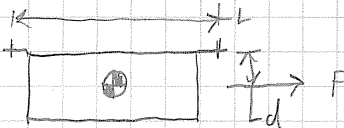
$$\text{Centroid} = \frac{\sum d^2}{N}$$

$$= \frac{(0.696)^2 \cdot (\sin^2 10 + \sin^2 20 + \sin^2 30 + \sin^2 40 + \sin^2 50 + \sin^2 60 + \sin^2 70 + \sin^2 80) \cdot 2 + (0.696)^2 \cdot \sin^2 90}{17}$$

$$\text{Centroid} = 0.223 \text{ m}$$

	SYSTEM: <i>Vista</i>	NAME: <i>Adkins</i>
	DRAWING NUMBER:	DATE: <i>29 May 04</i>
TOPIC: <i>Cassegrain Instrument Attachment</i>		PROJECT:
		PAGE: <i>4</i>

Find Force on Bolts due to Moments



Force Bolt = $\frac{Fd}{LN}$

For Circular Pattern use, SRSS of In-Plane Accelerations
Use distance between bolt centroids as L


$F = m \cdot a = 55,119 \text{ N}$ (shear force)


$L = 2(.223) = 0.446$

$d = 0.075 \text{ m}$

$N = 17$

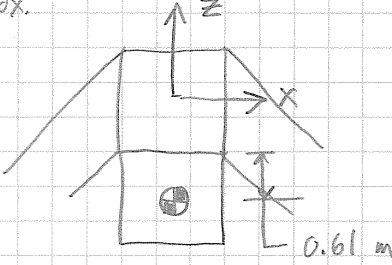
Force Bolt = 545 N

 <p>SYSTEM: Vista</p> <p>DRAWING NUMBER:</p>	NAME: Adkins
	DATE: 24 May 04
	PROJECT:
	PAGE: 5
<p>TOPIC: Cassegrain Instrument Attachment</p>	
<p>Find Complete Bolt Force</p> <p>⇒ Shear = 1,531 N</p> <p>Ten = 1,321 + 545 =</p> <p>⇒ Ten = 1,866 N</p> <p>Tension = Preload + (0.3) Ten</p> <p>Preload = 65,800 N (75% Yield)</p> <p>Tension = 65,800 + (0.3)(1,866)</p> <p>Tension = 66,360 N</p> <p>Find Interaction Equation</p> $\left(\frac{66,360}{87,700}\right)^2 + \left(\frac{1,866}{50,600}\right)^2 \leq 1$ <p><u>0.57 ≤ 1</u></p>	

 <p>Vertex RSI A TriPoint Global Company</p>	SYSTEM: Vista	NAME: Adkins
	DRAWING NUMBER:	DATE: 24 May 04
TOPIC: M2 Instrument Attachment		PROJECT:
		PAGE: 1

Determine the Bolt Forces and Interactions between the M2 Instrument and the mounting structure

Assume the M2 Instrument acts as the following rigid box.



Mass = 1,000 kg

M2 Accelerations @ MLE @ 94°

$X = 23.9 \text{ m/s}^2$ $Y = 13.6 \text{ m/s}^2$ $Z = 17.7 \text{ m/s}^2$

Find Bolt Shear Force (per connection)

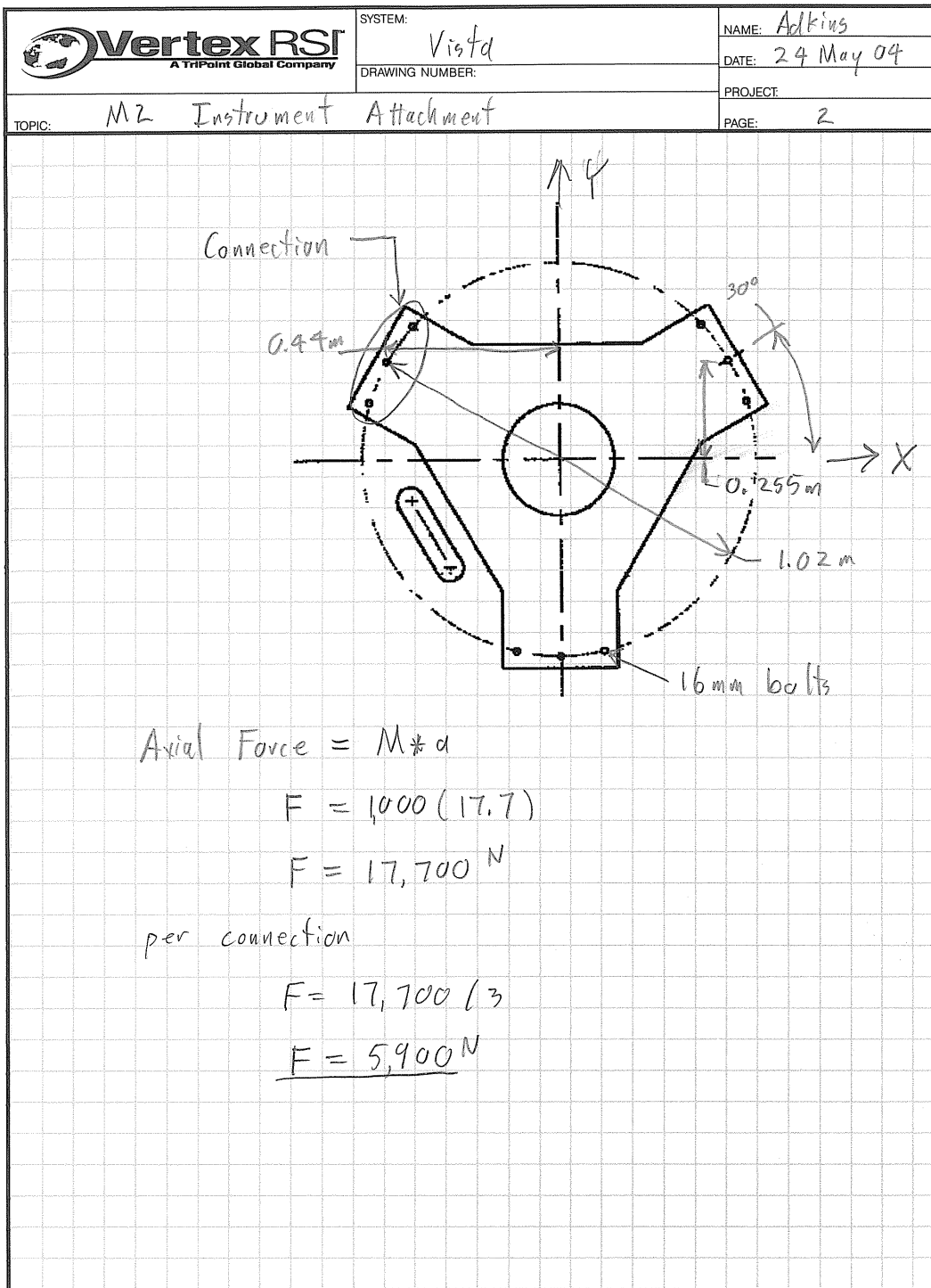
Shear Force = $M \cdot a$


$$F = 1000 (\sqrt{23.9^2 + 13.6^2})$$

$$F = 27,500 \text{ N}$$

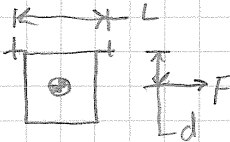
per connection

$$F = 27,500 \text{ N} / 3 = \underline{9,166 \text{ N}}$$



 <p>Vertex RSI A TriPoint Global Company</p>	SYSTEM: Vista	NAME: Adkins
	DRAWING NUMBER:	DATE: 24 May 04
TOPIC: M2 Instrument Attachment		PROJECT:
		PAGE: 3

Find Force on Bolts due to Moments



$$\text{Force Bolt} = \frac{Fd}{LN}$$

X Acceleration

$$F = m \cdot a = 1000(23.9) = 23,900 \text{ N}$$

$$d = 0.61 \text{ m}$$

$$L = (0.44) \cdot 2 = 0.88$$

$$N = 1$$


$$\text{Force Bolt} = 16,567 \text{ N}$$

Y Acceleration (N, d remain constant)

$$F = m \cdot a = 1000(13.6) = 13,600 \text{ N}$$

$$L = 0.51 + 0.255 = 0.765 \text{ m}$$

$$\text{Force Bolt} = 10,844 \text{ N}$$

 <p>Vertex RSI A TriPoint Global Company</p>	SYSTEM: <i>Vista</i>	NAME: <i>Adkins</i>
	DRAWING NUMBER:	DATE: <i>24 May 04</i>
TOPIC: <i>M2 Instrument Attachment</i>		PROJECT: <i>4</i>
<p>Find Complete Bolt Force</p> <p>Shear = $9,166 \text{ N}$ per connection</p> <p>shear = $9,166 / 3$ 3 bolts per connection</p> <p>⇒ Shear = $3,055 \text{ N}$</p> <p>Ten = $5,900 + 16,567 + 10,844$</p> <p>Ten = $33,311 / 3$</p> <p>⇒ Ten = $11,104 \text{ N}$</p> <p>Tension = Preload + $(0.3) \text{ Ten}$</p> <p>Preload = $122,500 \text{ N}$ (75% Yield)</p> <p>Tension = $122,500 + (0.3)(11,104)$</p> <p>Tension = $125,831 \text{ N}$</p> <p>Find Interaction Equation</p> $\left(\frac{\text{Ten}}{\text{Allow}}\right)^2 + \left(\frac{\text{shear}}{\text{Allow}}\right)^2 \leq 1$ $\left(\frac{125,831}{163,300}\right)^2 + \left(\frac{3055}{94,200}\right)^2 \leq 1$ <p style="text-align: center;"><u><u>$0.59 \leq 1$</u></u></p>		



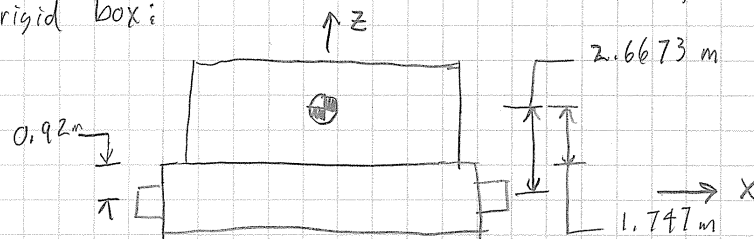
SYSTEM: Vista
DRAWING NUMBER:

NAME: Adkins
DATE: 24 May 04
PROJECT:
PAGE: 1

TOPIC: M2 structure to Elevation Ring

Determine the Bolt Forces and Interactions between the M2 structure and the Elevation Ring

Assume the M2 structure is the following rigid box:



$$\text{Mass} = 7893.9 \text{ Kg}$$

M2 Accelerations @ MLE @ 94°

$$X = 23.9 \text{ m/s}^2 \quad Y = 13.6 \text{ m/s}^2 \quad Z = 17.7 \text{ m/s}^2$$

Find Bolt Shear Force (per connection)

$$\text{Shear Force} = M \cdot a$$

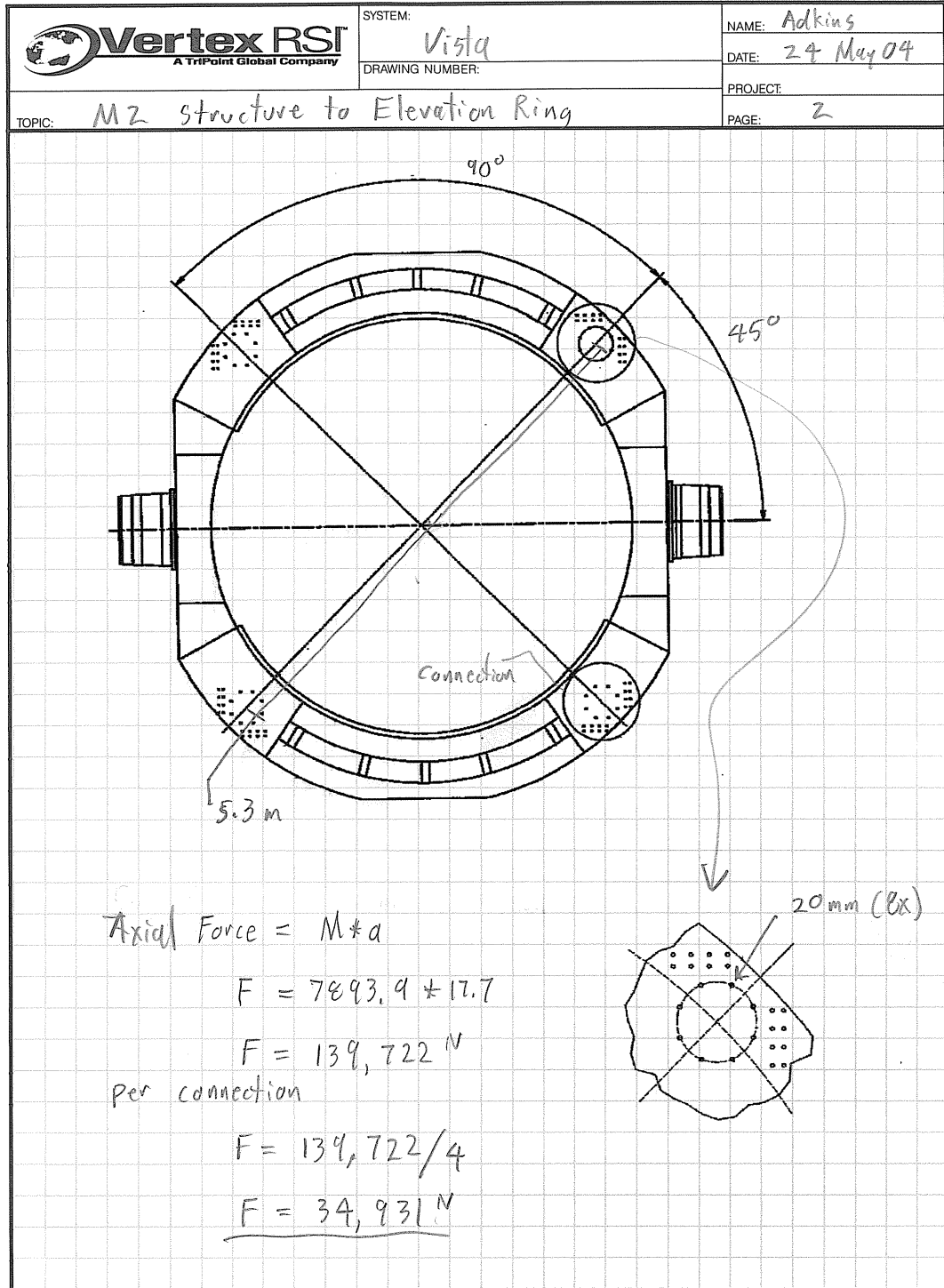
$$F = 7893.9 (\sqrt{23.9^2 + 13.6^2})$$

$$F = 217,071^N$$

per Connection

$$F = 217,071^N / 4$$

$$F = 54,268^N$$



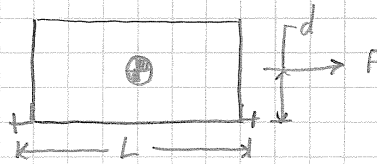


SYSTEM: Vista
DRAWING NUMBER:

NAME: Adkins
DATE: 24 May 04
PROJECT:
PAGE: 3

TOPIC: M2 Structure to Elevation Ring

Find Bolt Loads due to Moments



$$\text{Force Bolt} = \frac{Fd}{LN}$$

X Acceleration

$$F = M \cdot a = 7893.7 \cdot 23.9 = 188,660 \text{ N}$$

$$d = 1.747 \text{ m}$$

$$L = 5.3 \text{ m}$$


$$N = 2 \text{ connection}$$

$$\text{Force Bolt} = 31,093 \text{ N}$$

Y Acceleration (L, N, d remain constant)

$$F = M \cdot a = 7893.7 \cdot 13.6 \text{ m/s}^2 = 107,354$$

$$\text{Force Bolt} = 17,693 \text{ N}$$

 <p>Vertex RSI A TriPoint Global Company</p>	SYSTEM: Vista	NAME: Adkins
	DRAWING NUMBER:	DATE: 24 May 04
TOPIC: M2 Structure to Elevation Ring		PROJECT:
		PAGE: 4

Find Complete Bolt Force

$$\text{Shear} = 54,268 \text{ per connection}$$

$$\text{Shear} = 54,268 / 8 \text{ There are 8 bolts per connection}$$

$$\Rightarrow \text{Shear} = 6,784 \text{ N}$$

$$\text{Ten} = 34,931 + 31,093 + 17,693$$

$$\text{Ten} = 83,717 / 8$$

$$\Rightarrow \text{Ten} = 10,465 \text{ N}$$

$$\text{Tension} = \text{Preload} + (0.3)(\text{Ten}) \quad (\text{Preload} = 75\% \text{ Yield})$$

$$= 191,000 + (0.3)(10,465)$$

$$\text{Tension} = 194,140 \text{ N}$$

Find Interaction Equation

$$\left(\frac{\text{Ten}}{\text{allow}}\right)^2 + \left(\frac{\text{shear}}{\text{allow}}\right)^2 \leq 1$$

$$\left(\frac{194,140}{254,800}\right)^2 + \left(\frac{6784}{147,000}\right)^2 \leq 1$$

$$0.58 \leq 1$$



SYSTEM: Vista
DRAWING NUMBER:

NAME: Adkins
DATE: 29 May 04
PROJECT:
PAGE: 1

TOPIC: M1 Cell to Elevation Ring Connection

Determine the Bolt Forces and Interactions
between the M1 Cell and the Elevation Ring.

Find M1 Cell Mass and c.g.

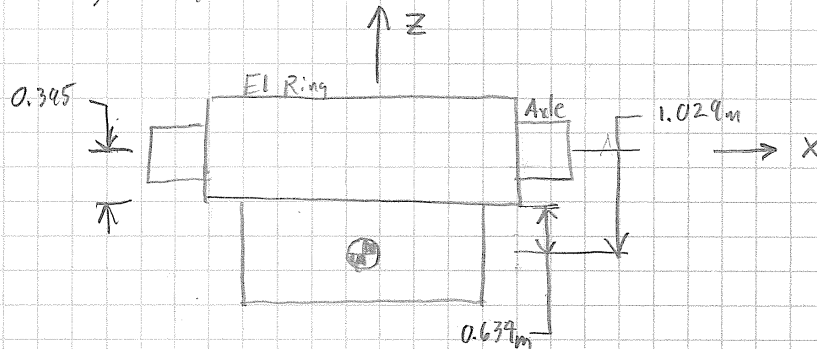
M1 Steel = 13,407 kg -1.0221 m

M1 Mirror = 5,520 kg -0.63382 m

Cassegrain = 2,900 kg -1.41442 m

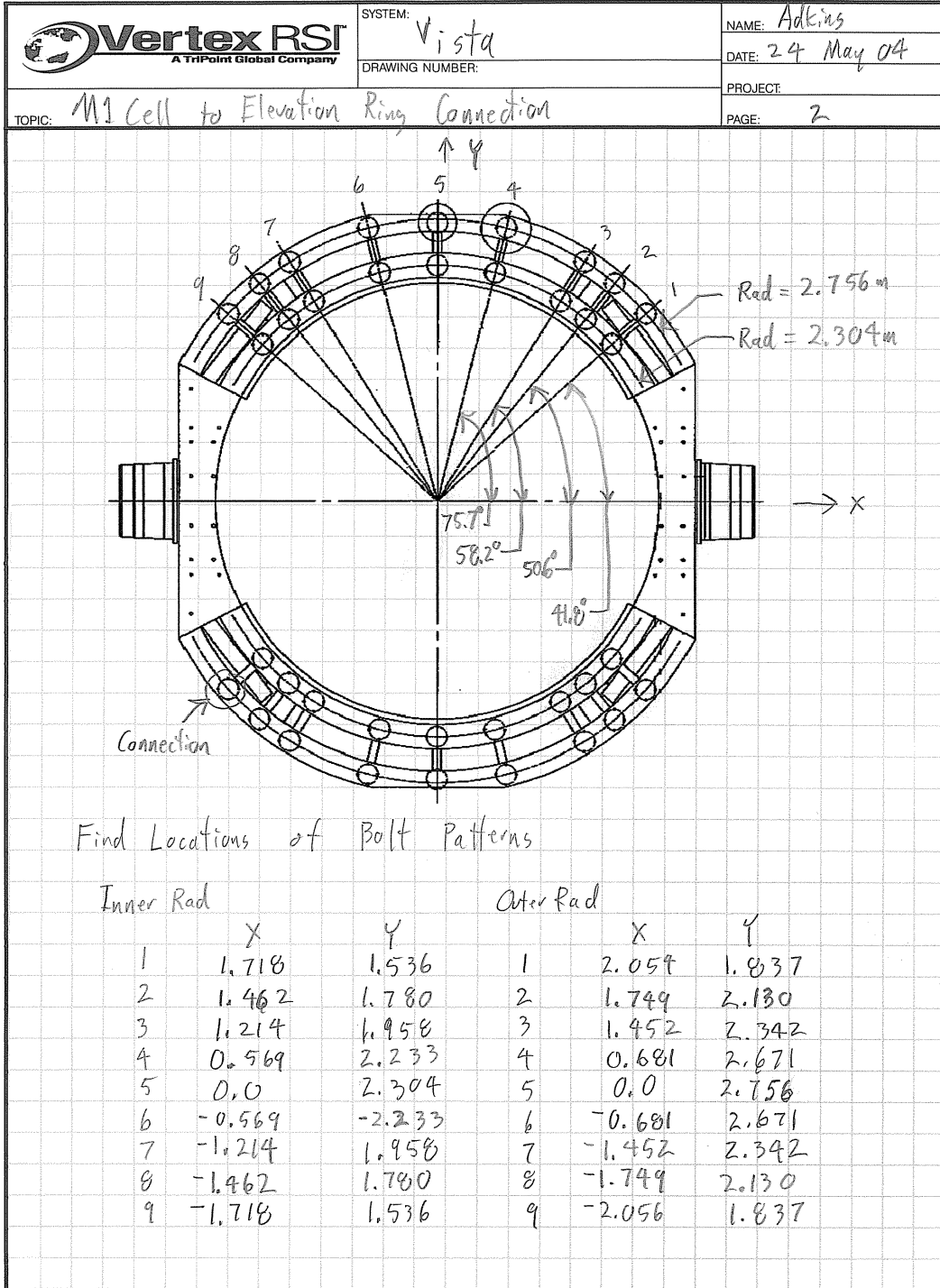
Total = 21,827 kg -1.029 m


Assume the M1 Cell is the following
rigid box:



M1 Accelerations @ MLE @ $\pm 4^\circ$

X = 14.0 m/s^2 Y = 13.5 m/s^2 Z = 15.2 m/s^2



 <p>SYSTEM: <i>Vista</i></p> <p>DRAWING NUMBER:</p>	NAME: <i>Adkins</i>
	DATE: <i>24 May 04</i>
TOPIC: <i>M1 Cell to Elevation Ring Connection</i>	PROJECT:
	PAGE: <i>3</i>

Find Bolt Forces: (Per Connection)

Shear $F = M + a$

$$F = 21,827 \text{ Kg} (\sqrt{14^2 + 13.5^2})$$

$$F = 424,506 \text{ N}$$

per Connection

$$F = 424,506 \text{ N} / 36$$

$$F_{\text{conn}} = 11,792 \text{ N}$$

Axial $F = M * a$

$$F = 21,827 \text{ Kg} (15.2)$$

$$F = 331,770 \text{ N}$$

per Connection

$$F = 331,770 \text{ N} / 36$$

$$F_{\text{conn}} = 9,216 \text{ N}$$

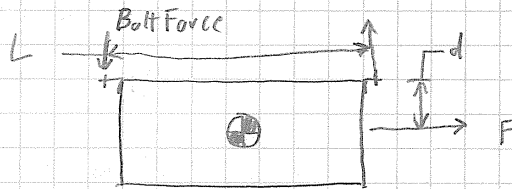


SYSTEM: Vista
DRAWING NUMBER:

NAME: Adkins
DATE: 29 May 04
PROJECT:
PAGE: 4

TOPIC: M1 Cell to Elevation Ring Connection

Find Bolt Loads due to Moments



$$\text{Bolt Force} = \frac{Fd}{L \cdot N} \quad \text{where: } N = \text{number of bolts}$$

X Acceleration:

$$F = M \cdot a_x = 21,827 \cdot 14 = 305,578 \text{ N}$$

$$d = 0.689 \text{ m}$$

$$L = 0.569 \cdot 2 \quad (\text{to be conservative, pick the smallest distance between bolt pairs})$$

$$N = 18$$

$$\text{Bolt Force} = \frac{305,578 \cdot 0.689}{1.138 \cdot 18}$$

$$\text{Force} = 10,204 \text{ N}$$

Y Acceleration: (d, N remain constant)

$$F = M \cdot a_y = 21,827 \cdot 13.5 = 294,665 \text{ N}$$

$$L = 1.536 \cdot 2 = 3.072 \text{ m}$$

$$\text{Force} = 3,645 \text{ N}$$



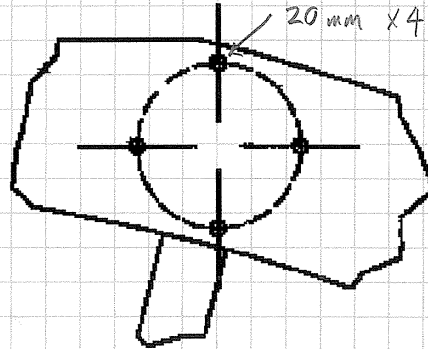
SYSTEM:
Vista
DRAWING NUMBER:

NAME: Adkins
DATE: 24 May 04
PROJECT:
PAGE: 5

TOPIC: M1 Cell to Elevation Ring Connection

Find Complete Force per Bolt

Each Connection
uses 4 20 mm
10.9 Bolts



$$\text{Tension} = 9,216 + 10,209 + 3,645 / 4$$

$$\Rightarrow \text{Tension} = 5,766 \text{ N}$$

$$\text{Shear} = 11,792 / 4$$

$$\Rightarrow \text{shear} = 2,948 \text{ N}$$

$$F_{\text{Ten}} = F_{\text{Preload}} + (0.3)(F_{\text{Ten}})$$

$$F_{\text{Preload}} = 75\% \text{ Yield} = 191,100 \text{ N}$$

$$F_{\text{Ten}} = 191,100 + (0.3)(5,766) = 192,830 \text{ N}$$

Interaction Equation

$$\frac{F_{\text{Ten}}}{F_{\text{TenAllow}}}^2 + \frac{F_{\text{Shear}}}{F_{\text{ShearAllow}}} \leq 1$$

$$\left(\frac{192,830}{254,800}\right)^2 + \left(\frac{2,948}{147,000}\right)^2 = 0.57 \leq 1$$



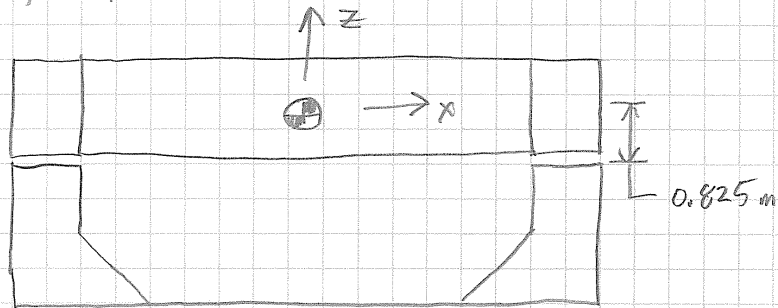
SYSTEM: Vista
DRAWING NUMBER:

NAME: Adkins
DATE: 24 May 04
PROJECT:
PAGE: 1

TOPIC: Elevation Bearing Housing Attachment

Determine the Bolt Forces and Interactions
between the Elevation Bearing Housings and the Yoke.

Assume the OSS and the Housings acts as the
following Rigid Box



$$\text{Mass} = 49,325 \text{ Kg}$$

OSS Accelerations @ MLE @ 94°

$$X = 16.3 \text{ m/s}^2 \quad Y = 12.3 \text{ m/s}^2 \quad Z = 17.4 \text{ m/s}^2$$

Find Bolt Shear Force

$$\text{Shear Force} = M \cdot a$$

$$F = 49,325 (\sqrt{16.3^2 + 12.3^2})$$

$$F = 1,007,221 \text{ N}$$

per bolt

$$F = 1,007,221 \text{ N} / 16 = 62,951 \text{ N}$$



SYSTEM: *Vista*

NAME: *Adkins*
DATE: *24 May 04*

DRAWING NUMBER:

PROJECT:

TOPIC: *Elevation Bearing Housing Attachment*

PAGE: *2*

Axial Force = $M \cdot d$

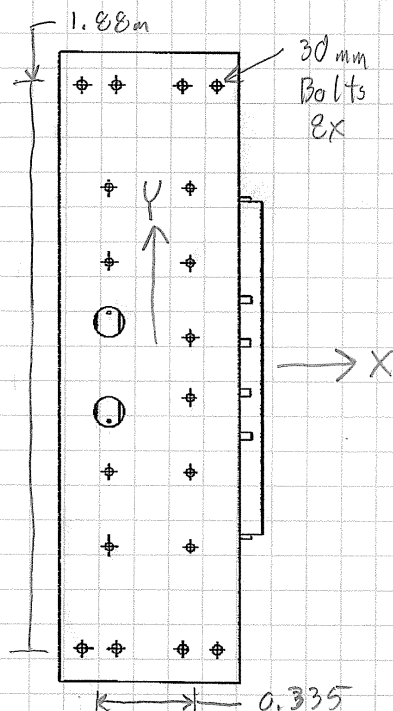
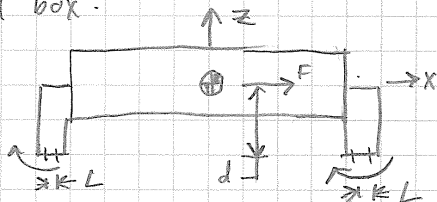
$$F = 49,325(17.4)$$

$$F = 858,255 / 16 \text{ bolts}$$

$$F = 53,641 \text{ N}$$

Find Bolt Forces due to Moments

Assume the OSS is the following rigid box:



X Acceleration


$$F = m \cdot a = 49,325(16.3) = 804,000 \text{ N (Symmetric)}$$

$$L = 0.335$$

$$d = 0.825$$

$$N = 8 \text{ (4 per housing)}$$

$$\text{Force Bolt} = 247,500 \text{ N}$$

 <p>Vertex RSI A TriPoint Global Company</p>	SYSTEM:	NAME: <i>Adkins</i>
	DRAWING NUMBER:	DATE: <i>24 May 04</i>
TOPIC: <i>Elevation Bearing Housing Attachment</i>		PROJECT:
		PAGE: <i>3</i>

Y Acceleration:

$$F = m * a = 49,325 (12.3) = 606,700 \text{ N}$$

$$L = 1.88 \text{ m}$$

$$d = 0.825 \text{ m}$$

$$N = 8$$

$$\text{Force Bolt} = 33,280 \text{ N}$$

Find Complete Bolt Force

$$\Rightarrow \text{Shear} = 62,951 \text{ N}$$

$$\Rightarrow \text{Ten} = 53,641 + 247,500 + 33,280 = 334,420 \text{ N}$$

$$\text{Tension} = \text{Preload} + (0.3)(\text{Ten})$$

$$\text{Preload} = 437,600 \text{ N} \quad (75\% \text{ Yield})$$

$$\text{Tension} = 437,600 + (0.3)(334,420)$$

$$\text{Tension} = 537,926 \text{ N}$$

Find Interaction Equation

$$\left(\frac{537,926}{583,400} \right)^2 + \left(\frac{62,951}{336,000} \right)^2 \leq 1$$

$$\underline{\underline{0.89 \leq 1}}$$